Suitability of Self-Reducing and Slag-Forming Briquettes for EAF Use based on Laboratory Tests

Ahmed Abdelrahim*, Matti Aula, Mikko Iljana, Thomas Willms, Thomas Echterhof, Stefan Steinlechner, Davide Mombelli, Carlo Mapelli, Mamdouh Omran, Stefan Preiss and Timo Fabritius

Affiliations:

A. Abdelrahim, M. Aula, M. Iljana, M. Omran, T. Fabritius

Process Metallurgy Research Unit,

University of Oulu, Pentti Kaiteran katu 1, 90014 Oulu, Finland

T. Willms, T. Echterhof

Department for Industrial Furnaces and Heat Engineering, RWTH Aachen University, Kopernikusstr. 10, 52074 Aachen, Germany

S. Steinlechner

Chair of Nonferrous Metallurgy, Montanuniversitaet Leoben, Franz-Josef-Str. 18, 8700 Leoben, Austria

D. Mombelli, C. Mapelli

Dipartimento di Meccanica, Politecnico di Milano, Via La Masa 1, 20156 Milano, Italy

S. Preiss

MFG Metall- und Ferrolegierungsgesellschaft mbH Hafner, Blondin & Tidou, Rudolf-Diesel-Str. 9, 40670 Meerbusch, Germany

* Corresponding author email: ahmed.abdelmonem@oulu.fi

Keywords:

EAF, Briquetting, Recycling, High temperature tests

Abstract

This article has been accepted for publication and undergone full peer review but has not been through the copyediting, typesetting, pagination and proofreading process, which may lead to differences between this version and the Version of Record. Please cite this article as doi: 10.1002/srin.202100472.

The in-plant recycling routes of several side streams produced in Electric Arc Furnace (EAF) steelmaking remain under-explored. Briquetting is an attractive technique to enable recycling of in-plant side streams. Briquettes introduced into EAF must possess certain mechanical and chemical properties. However, no standard is available to determine the suitability of briquettes used in the EAF process. In this work, eight side streams were characterized, and used to produce seven different briquettes to be used in EAF. Side streams were obtained from three different EAF steel plants as well as two other industrial sites. Briquettes tested consisted of four self-reducing briquettes and three slag-forming briquettes produced using different recipes. The briquettes were subjected to several mechanical and thermal tests which reflect their intended use in EAF. The mechanical tests included compression and drop tests, and the thermal tests included optical dilatometry, TGA-DTG-MS, and full-scale briquette reduction tests. Moreover, melting trials were performed to assess the melting behavior of selected briquettes and their interaction with slag. Suitability of briquettes characteristics were assessed based on values from literature and against reference ferroalloys and lime stones used in one of the steel plants. Two briquettes were deemed suitable for EAF use, while three briquettes were deemed unsuitable, and two briquettes were considered of limited use.

1. Introduction

In 2020, 26.3% of crude steel was produced through the electric steelmaking route.[1] Several waste streams are generated in high quantities when steel is produced using an Electric Arc Furnace (EAF), and some of this waste is considered hazardous.[2] The amount of slag, dust, and sludge generated during the EAF process is an estimated 181.4 kg per ton of crude steel produced.[3] Side streams used in this study are obtained from three different EAF steelmaking plants as well as two other industrial sites. The main side streams originating from one of the steelmaking plant amounts to 122490 tons per year, the breakdown of which is shown in Table 1 below.

Table 1 Main side steams from a steelmaking plant.

Side stream	Quantity (ton per year)
EAF Slag	60896
Secondary metallurgy slag	23262
MgO-C refractories	2495
Alumina refractories	184
EAF and LF Dust	14087
Combustion chamber Dust	1994
Wet and dry Mill Scale	12058
Oxi-cutting fines	Not reported
Fines from EAF belt additions	2880
Fines from LF belt additions	204
Sludge from water treatment	1093
Mud pit*	3337

*Sludge from tanks cleaning is collected in mud pit outside of the plant

Steel production via EAFs is expected to increase in the future (and, thus, the volume of generated waste) due to increasing recycling volumes and the transition to hydrogen-based reduction. Moreover, the process is associated with lower capital costs and higher process flexibility.[4,5] Several techniques have been investigated to recover valuable elements from EAF side streams.[6] Beneficiation techniques used on EAF side streams include thermal and hydrometallurgical methods.[7] Common methods include leaching and the use of a Waelz kiln to recover zinc and other valuable metals from dust particles. However, to become economically viable, the waste stream should be adequately large with high metal content to be extracted.[2] Briquetting is one of the techniques used to incorporate side streams into the production cycle in steel plants.[8] The general costs of EAF processes could be cut by replacing expensive charge materials with cheaper side stream-based ones.[9] Furthermore, the internal recycling of side streams into EAF processes decreases the potential costs associated with the disposal of the side streams.

Researchers have demonstrated the feasibility of utilizing briquettes produced using side streams in EAF steelmaking with the purpose of recycling metal oxides and creating slag foaming.[10–13] Several testing standards are used to assess iron-bearing materials quality and suitability for a blast furnace (BF). The parameters assessed include chemical composition, cold strength, reducibility and softening and melting properties.[14] However, utilizing briquettes in an EAF is not as highly standardized.

In this research, selected analysis methods for different briquettes are chosen to reflect their intended use in an EAF. Mechanical properties are compared against reference materials used in EAF. Thermal characteristics are assessed employing laboratory testing techniques to evaluate the suitability of four self-reducing briquettes as well as three slag forming briquettes to be used in EAF.

2. Requirement and testing of cold bonded briquettes for their use in EAF.

Steelmaking production via the EAF route involves handling the input, charging the batch, melting, and refining.[3] The briquettes used in EAF are subject to different forces in these phases, and the briquettes behavior in these phases should be evaluated.

2.1. Handling and charging of EAF burden material

The briquettes to be used in EAF need to be able to withstand handling at the scrap yard or feeding through a silo. The briquettes can be charged to EAF either through the scrap basket or a charging chute in the EAF's roof. The minimum mechanical strength requirement of the briquette is that it does not crumble during handling, or under the load of the basket.

A standard is available to determine the crushing strength of iron ore pellets.[15] However, no standard is available for the testing of briquettes. In compression tests, researchers determine the strength of briquettes after curing durations that could vary from 1 to 28 days after production.[16–18] The number of tested briquette samples and acceptable strengths also vary; Richards [19] reported that industrial briquettes should have a minimum compression strength of 350 kPa, which corresponds to the maximum stress that takes place during the loader bucket filling, while Kumar et al.[20] suggested a minimum strength of 100 kg/briquette. López and López-Delgado[21] evaluated the mechanical properties of briquettes through tumbler testing based on ISO standards.[22] They considered a tumbler index higher than 55% to be acceptable for briquette handling, although the optimum tumbler index is considered to be 70% and 90% for sinters and pellets, respectively.[14]

2.2. Charging

The briquettes to be utilized in an EAF are required to withstand the mechanical stress associated with the introduction of briquettes to EAF. Drop damage resistance is of high importance since it has been suggested that direct fly-off following the charging procedure in an EAF is one of the main contributors to dust generation.[23] Drop damage resistance can be evaluated by dropping a briquette from a certain height onto a steel plate and observing the mass loss of the dropped briquette. Jarnerud et al. [24] compared the drop test results of briquettes to those of lime lumps used in EAFs and determined that a briquette should withstand 7–9 drops in industrial conditions. However, the specifics of the conducted drop tests differ significantly. While El-Hussiny and Shalabi [17] chose to drop the briquettes from a height as low as 0.3 m, Mousa et al.[25] evaluated briquettes by dropping them from a height of 1 m, Magdziarz et al. [18] and Demus et al.[26] dropped the briquettes from a height of 2 m, and Paknahad et al.[27] dropped them from a height of 4 m. Drop damage resistance is

expressed as the number of drops before breakage or as a percentage based on the fines generated. Similar to compression tests, a drop test is carried out after curing for up to 28 days.[17,25] It should be pointed out that for a cupola furnace, the briquettes must withstand dropping from a 1 m height.[28] It can be argued that since the briquettes will be charged to furnace, the minimum drop height the briquettes should withstand is the approximate height of the scrap basket when it opens, which is in the range of a few meters. Unfortunately, no standards are available for drop tests, which leads to the lack of both specific procedures, dropping height and threshold values to assess the suitability of a briquette. The only available standards for drop shatter testing are related to coal and coke.[29,30] For coal and coke testing, a heigh of 1.63 m is indicated, and the cumulative mass fraction retained by specified sieves must be declared. Furthermore, for coal, size stability and friability indexes must be calculated to accurately determine the tested portion's tendency toward fragmentation. Blesa et al.[31] and Sen et al.[32] suggested that other parameters could better describe the drop behavior of a briquette. One of these parameters is the Impact Resistance Index (IRI), which is calculated by dividing the number of drops of each briquette by the number of pieces it splits into. The other parameter is the Adjusted Impact Resistance Index (AIRI), which also considers the amount of powder detached during the drop test. All these examples could be integrated into a specific procedure or standard to characterize the mechanical behavior of EAF briquettes.

2.3. Heating in the scrap charge

The briquettes charged in the basket are subject to high-temperature gases arising from the arc, melt pool, and burners. The minimum requirement for the briquettes is to retain their shape during the heating process without generating an excessive number of fine particles. Furthermore, briquettes containing oxide components are expected to somewhat reduce while they are heated in a reducing atmosphere. Changes in the sample shape during heating can be measured with optical dilatometry. The aim of dilatometry trials is to analyze how briquettes retain their shape during heating. The softening and melting temperatures of the briquette can then be evaluated if they meet the criteria for their intended use.

Several researchers have studied the heating of composites containing FeO and polymeric blends in a laboratory-scale horizontal tube furnace equipped with a camera to monitor physical changes in the composite, similar to an optical dilatometer.[33–35] López and López-Delgado [21] determined the softening, start of melting, and complete melting temperature of briquettes using a Leitz Wetzlar heating microscope with temperature up to 1500 °C. According to Babanin et al.[36], briquettes should possess adequate thermal strength up to 500 °C to be suitable for ferrous metal production. Low-temperature disintegration is obtained by measuring the pellet-size distribution after static reduction at 500 °C, followed by tumbling. This method was employed by Lemos et al.[37] to test briquettes based on standard ISO 4696-1 (Iron Ores–Static Test for Low-Temperature Reduction Disintegration).[38] Also, the decrepitation test, still derived from the iron ore standard, can be applied to investigate the thermal behavior of briquettes for EAF purposes.[39]

Current tap-to-tap times in EAFs are well below 1 h, depending on the grade produced.[40] Furthermore, the length of time in which the batch is heated, but not yet molten, can be short. This period occurs after the electrodes are bored in the scrap batch and before all the scrap on the sides has become molten. Therefore, briquettes intended for use in an EAF have a limited time for direct reduction. The reduction behavior of briquettes is conventionally tested by thermogravimetry tests at different temperatures and expressed as the fraction of reduced oxygen over the total reducible oxygen.[10] In these trials, it is important to consider the size of the briquette and heating rate, as heat transfer has been found to be a controlling step.[10]

2.4. Evolving gases

The effect on off-gas composition and dust formation is evaluated when adding new materials to an EAF is planned. The briquettes introduced to EAF should not excessively increase the dust load through volatilization neither should they increase the amount of hazardous compounds in off-gases. The amount of alkali compounds in the briquettes cannot be excessive, or alkali accumulation on the off-gas duct may occur. Furthermore, volatilizing chlorine can cause significant corrosion of the off-gas duct. Although the carbon content of a briquette may be beneficial as an external energy source and combined with the oxygen injection in an EAF, the charge of some carbon-bearing material may result in the emission of benzene, toluene, and xylenes.[41] López and López-Delgado [21] assessed the lead, zinc, and alkali chloride gases output products resulting from the use of briquettes using Outokumpu HSC Chemistry software[42] simulation, while Ye et al.[43] assessed chlorides and zinc output resulting from briquettes by collecting and analyzing volatilized matters during briquette reduction.

2.5. Melting behavior

After the scrap becomes molten, the briquettes are in direct contact with molten slag. During this period, the further reduction of FeO occurs, but it is limited by the kinetics and the amount of carbon in the steel melt. When charging briquettes prepared from spent refractory, it is important to consider the dissolution of the briquettes in molten slag. In cases of large briquettes and slow dissolution, the unmolten briquettes can potentially clog the tapping hole of the EAF during tapping.

Briquettes potentially used in EAF are typically tested in pilot-scale melting trials. Demus et al.[26] conducted melting trials in a pilot-scale EAF using briquettes produced from biochar fines. In the study, 1.79 kg of biochar briquettes was charged per 50 kg of scrap and slag former. The use of briquettes showed no negative effect on either the melt or slag with regard to chemical composition. The combustion behavior of the briquettes was investigated through the analysis of off-gases, and it was concluded that the CO formation rate was relatively high in biochar briquettes. Willms et al.[44] conducted pilot-scale trials using 45 L a direct current electric arc furnace to assess the dissolution behavior of briquettes in melt pool and determined changes in the steel and slag phase. Takano et

al.[45] evaluated the metallic yield of briquettes by charging 1 kg of agglomerates into a 2.8 kg of Fe-C liquid melted and kept at 1500 °C and then weighing the metal after solidification.

In the present article, a summary of the methods used to assess the behavior of briquettes in an EAF is presented in Table 2. Various briquettes characteristics are evaluated using the methods shown

Table 2: Summary of methods applied to assess various phenomenon.

Process step	Test	Assessment
Charging and handling	Compression test	Assessment of briquettes' ability to withstand storage, handling, and charging in a basket.
	Drop test	Assessment of dust generation after being charged in an EAF.
Heating of briquette	Thermogravimetric analysis (TGA) coupled with mass spectrometry (MS)	Determining stages of binder disintegration, carbon gasification and iron oxides reduction. Assessment of potential unwanted produced gases e.g., benzene, toluene and xylenes.
	Dilatometer	Softening behavior of briquettes from the first basket introduced to the EAF.
	Full scale briquette TG	Assessment of the initial reduction degree of full-scale briquettes.
Melting of briquettes	Melting and dissolution trial	Interaction of freshly charged briquettes with melt (e.g., briquettes from second or third basket with the melt from first basket).

3. Materials and Methods

3.1. Side streams

Eight different side streams as well as coal injection were used in this study to produce briquettes. materials were obtained from three different EAF steelmaking plants and two industrial facilities. The origin of each side stream is shown in Table 3 below.

Table 3 Origin of side streams used in briquettes production.

Side stream	Origin
Ladle furnace slag_1	Collected from plant No.1 secondary metallurgy ladle furnaces.
Ladle furnace slag_2	Collected from plant No.2 secondary metallurgy ladle furnaces.
Mixed residues	Collected in plant No.2 and consist of mixture of different remaining materials which are generated in the steel plant (from metallurgical hall to the rolling mill).
Belt Conveyor Fines	Collected in plant No.3 and consists of mixture of different materials which are added through the belt conveyor in the EAF and are rich in CaO.
Oxy-cutting Fines	Collected in plant No.3 from the off gases coming from the cutting of the billets in the continuous casting area
Combustion Chamber Dust	Collected in plant No.3 in a box in the combustion chamber at the off-gas duct, where the remaining combustible components of the off-gases are post combusted.
Grinding Sludge	Collected from a bearing manufacturer near plant No.3
Ferromanganese Carbon dust	Consists of filtering system dusts from FeMnC production site.

As received samples of the side streams are shown in Figure 1 below. Oxy-cutting fines appear dusty, easily compactable and brown. No coarse particles were detected. EAF fines appeared to be silky, white powder, easily compactable. No coarse fraction was detected as well. Grinding sludge samples were in the form of matt grey, smelly powder with some friable coarse blocks. Ladle furnace slag_1 appeared to be in a form of dark brown-grey blocky-shaped material with a size range of a few millimeters, but with some very coarse blocks. Ladle furnace slag_2 slag was a smooth light grey powder with some coarse particles within.

(a) (b) (c) (d) (e)

Figure 1 As received samples showing oxy-cutting fines (a), belt conveyor fines (b), grinding sludge (c), ladle furnace slag_1 coarse fraction (d), ladle furnace slag_2 fine fraction (e).

Moisture content of side streams was determined by heating samples overnight at 105°C according to the standard EN 14346:2006.[46] The bulk and true density of side streams were determined according to standards EN 1097:1998 and BS EN 1097-7:2008, respectively.[47,48] The moisture content, and densities of side stream used are shown in Table 4 below.

Table 4 Moisture content (-wt% on wet basis), bulk density and true density of side streams used in briquettes making.

Material	Moisture content (%)	Bulk density (g/cm^3)	True density (g/cm^3)
Ladle furnace slag_1	0.18	1.32	3.24
Ladle furnace slag_2	0.00	1.24	3.33
Mixed residues	13.56	1.51	2.93
Belt conveyer fines	-	1.03	3.66
Oxy cutting fines	4.73	1.82	4.74
Combustion chamber dust	6.40	2.19	4.28
Grinding sludge	24.79	1.19	5.30
Ferromanganese Carbon dust	3.98	0.75	3.23

At a pre-processing stage, as received side stream materials were crushed and sieved if necessary to obtain a particle size that is less than 4 mm, a size which was empirically decided.[44] As received ladle slag_1, for example, contained large chunks that were not suitable for Particle Size Distribution (PSD) analysis. To determine PSD of the material, two techniques were used. A laser granulometer mastersize 2000 was used to determine the PSD for briquettes fine components, oxy-cutting fines and belt conveyor fines. As a preparation step, the samples were dispersed in Isopropanol and treated for 1 minute with ultrasonic. PSD of oxy-cutting fines and belt conveyor fines are shown in Figure 2. It is clear that both materials are dominated by very fine particles with D50 of oxy-cutting fines and belt conveyor fines being 6.68 and 7.91 µm, respectively.

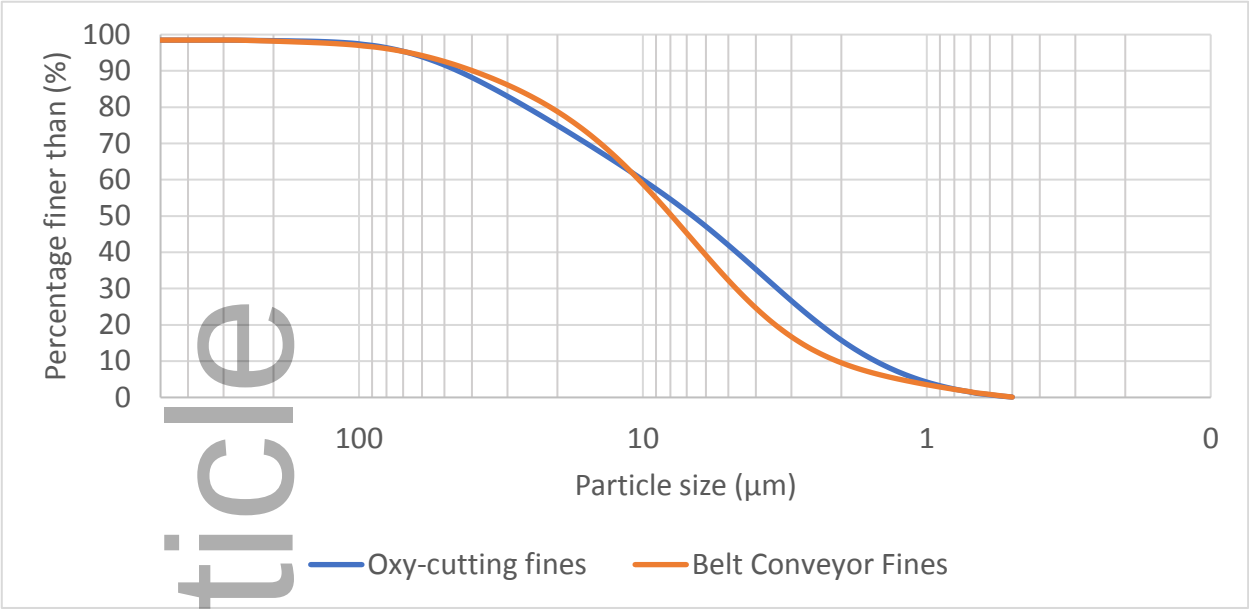

Figure 2 PSD of Oxy-cutting fines and belt conveyor fines determined by laser granulometer mastersize 2000

To determine the PSD of coarser material, sieving technique was used. PSD of combustion chamber dust and mixed residues are shown in Figure 3. It appears that both materials have coarse PSD when compared to oxy-cutting fines and belt conveyor fines, with combustion chamber dust and mixed residues having a D50 of 0.78 and 0.82 mm, respectively.

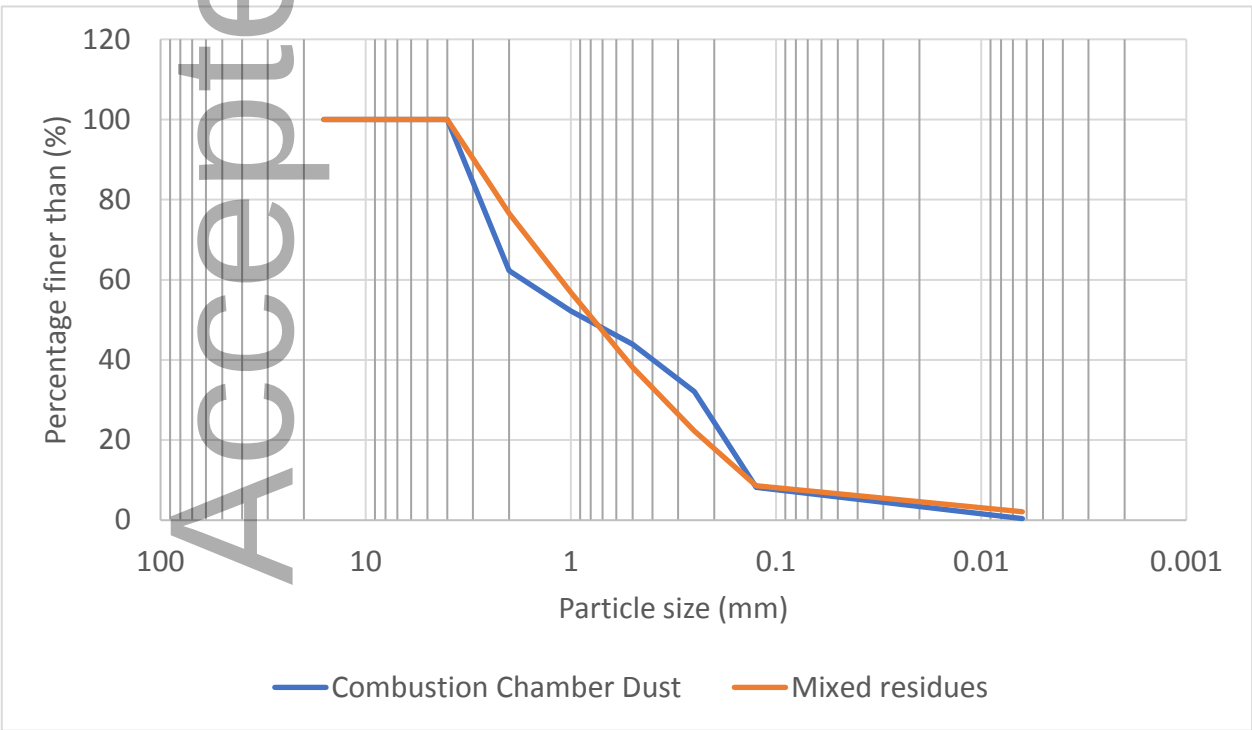

Figure 3 PSD of combustion chamber dust and mixed residues determined by sieving.

PSD distribution plays a major role in the briquette's quality. It was reported that suitable feed material used in cold bonding should have at least 80% of the total feed being finer than 200-250 μm.[49] It was also reported that utilization of finely ground material in briquettes results in compaction increase and ultimately higher briquette strength.[50] However, others reported that an increase of the fine fraction of fine material in briquettes beyond 30% may lead to a deterioration in briquettes strength or increased use of binder, and a balance between finer and coarser fraction should exist within PSD of briquettes.[20]

To determine the chemical composition of side streams, X-ray Fluorescence Analysis (XRF) was carried out using a Philips PW 2404 with an energy dispersive X-Ray fluorescence detector. In order to prepare side stream samples, they were milled to reduce the grain size and obtain homogenous samples. Eight grams of each side stream material were mixed with two grams of tableting aid, Hoechst wax C micropowder and pressed under 150 kN. The results of chemical composition of the side streams are shown in Table 5 below.

Table 5 Chemical composition of side streams used in briquettes making.

Material	Al_2O_3	CaO	Cr_2O_3	MgO	MnO	P_2O_5	S	SiO_2	Fe_2O_3
Ladle furnace slag_1	8.27	46.65	0.04	11.74	1.98	0.50	0.38	27.52	1.42
Ladle furnace slag_2	11.23	50.61	0.17	9.83	0.56	0.48	1.22	21.18	2.08
Mixed residues	14.07	37.93	0.53	13.99	2.76	0.61	0.63	14.82	11.84
Belt Conveyor Fines	0.21	90.08	1.06	0.99	1.45	0.33	0.21	2.97	1.75
Oxy-cutting Fines	0.17	1.29	0.65	0.36	0.81	0.53	0.18	1.06	92.72
Combustion Chamber Dust	1.91	9.30	1.28	1.95	3.45	0.63	0.19	4.38	64.09
Grinding Sludge	1.06	0.15	1.73	0.10	0.32	0.43	0.08	3.57	92.09
Ferromanganese Carbon dust*	1.89	5.61	-	3.38	58.81	0.06	-	9.65	2.67

* Rest in wt.- %: 9.86 K_2O; 3.90 Na_2O; 0.99 Cl.

Side streams rich in iron were then characterized for their total iron content employing standard DIN EN ISO 1188. Metallic iron was determined employing standard ISO 5416. The Fe^{2+} content was determined using titration method AM_EG.26, and finally, Fe^{3+} was calculated. Table 6 shows the iron content analysis of grinding sludge, oxy cutting fines and combustion chamber dust. Grinding sludge is rich in metallic iron, and total iron content, making it very attractive to be recycled back to EAF. Oxy cutting fines is also rich in iron, but it mostly exists as iron oxides. Combustion chamber dust contained significant amount of iron also that mostly exists as oxide. XRD analysis results reported previously[16], confirmed the most abundant phase in griding sludge is metallic iron, and in oxy-cutting fines is magnetite. In combustion chamber dust, the most abundant phases were brownmillerite, franklinite, goethite, and finally plumboferrite.

Table 6 Iron content analysis of iron rich-side streams

Material	Fe total	Fe^{2+}	Fe^{3+}	Fe met
Grinding sludge	83.60	24.10	0.30	59.20
Oxy cutting fines	68.20	16.40	51.50	0.30
Combustion chamber dust	45.10	16.40	26.90	1.80

3.2. Briquettes making

Two briquetting machines, Gabbrielli L-4 stamp press with 73 mm round mould and Carver stamp press with a 49.5 mm round mould were used to produce briquettes. In preliminary briquetting trials, different briquetting parameters were tested. Several briquetting parameters affect the quality of produced briquettes. These parameters include particle size distribution, briquetting force, mixing procedures, chemical composition of briquettes components, moisture content and binder used.[20,50]

Briquetting parameters tested in this work included binders used such as starch, molases, sodium silicate, polyethylenglycol (PEG) and carboxymethylcellulose (CMC). Other briquetting parameters investigated included clearance between mould and upper stamp (50-500 µm), moisture content, fibres from paper recycling and manufacturing pressure (10-40 MPa). Based on preliminary tests, a total of six briquettes were produced using Gabbrielli L-4 stamp press, and one briquette recipe, BRIQ4 was produced using Carver stamp press. Briquettes were cured in ambient atmosphere and temperature for at least 10 days before subsequent mechanical tests, except for BRIQ4 which was also tested for early development of mechanical strength on the second and seventh day of production. The procedures used for briquettes making and recipe optimization can be found in previous publications.[16,44]

The behavior of the seven different briquettes were evaluated for their use in an EAF through different tests. Four of the briquettes were intended to self-reduce in an EAF, so they contained high levels of iron oxides and carbon (BRIQ1, BRIQ3, BRIQ4, BRIQ5). Briquettes BRIQ2, BRIQ6, and BRIQ7 were intended to support the formation of slag in an EAF, so they contained high levels of CaO and significant amounts of MgO. Starch was mainly employed as a binder in all briquettes except for BRIQ6 which contained both starch and sodium silicate as binders. Moisture content of briquettes originated from side streams moisture content as well as water added during briquettes production. Briquettes' recipes are presented in Table 7. A significant advantage of cement-free briquettes is that they require less energy to melt than cement-bonded briquettes.

Table 7 Briquette's recipe (-wt% on wet basis)

Material	BRIQ1	BRIQ2	BRIQ3	BRIQ4	BRIQ5	BRIQ6	BRIQ7
Ladle furnace slag_1	-	-	-	-	-	80.90	-
Ladle furnace slag_2	-	-	-	-	-	-	44.10
Mixed residues	-	-	-	-	-	-	44.10
Belt Conveyor Fines	-	63.40	-	-	-	-	-
Oxy-cutting Fines	36.20	-	33.80	33.80	-	-	-
Combustion Chamber Dust	35.90	-	-	-	-	-	-
Grinding Sludge	-	-	46.00	43.10	-	-	-
Ferromanganese Carbon dust	-	-	-	-	69.70	-	-
Coal Injection	15.60	-	10.20	10.20	8.40	-	-
$Ca(OH)_2$	-	-	-	-	2.40	-	-
Paper fibers	0.90	0.70	0.90	1.90	1.00	-	0.90
Starch	4.00	4.80	9.20	11.00	6.90	5.00	8.80
Sodium Silicate	-	-	-	-	-	14.10	-
External water added	7.40	31.10	-	-	11.70	-	2.20

When taking the moisture content of briquettes components into account, the moisture content of the briquettes could be calculated. Final moisture content of briquettes is shown in Table 8.

Table 8 Final moisture content of produced briquette on wet basis (-wt%)

Briquette	BRIQ1	BRIQ2	BRIQ3	BRIQ4	BRIQ5	BRIQ6	BRIQ7
Total moisture content	11.41	31.10	12.90	12.28	11.60	7.20	8.08

During curing, part of the moisture content evaporates, and part of it would react, mostly with binders to form the binding matrix. Mass loss of eight briquettes from BRIQ4 recipe was recorded during the course of first week of curing. After one week of curing, briquettes mass loss range was between 1.45 - 1.96 grams with an average of 1.70 grams. The mass loss of briquettes was accompanied by a 2.14% volume shrinkage.

Briquettes produced had cylindrical shape. Briquettes dimensions were measured after at least 7 days of curing. Briquettes' height of each recipe varied depending on briquetting parameters employed. All the briquettes were manufactured with a diameter of 72.6 ± 0.3 mm except for BRIQ4 which had a diameter of 49.9 ± 0.1 mm as it was manufactured using a different lab press and die briquetting machine.

For easier interpretations and more comparable results, one briquette of each recipe was cut into several (1 cm^3) cubes. Cubes from the same briquettes were used for skeletal density measurements, dilatometry analysis, TGA-MS analysis and melting trials. Cutting of samples was done using Struers Secotom-10 with a 1 mm diamond composite cutting wheel. Cutting wheel rotation speed was 4000 rpm at a feed speed of 0.25 mm s^{-1}. Water was used as a cutting fluid. When attempting to cut the briquettes and prepare them for testing, samples from BRIQ5, BRIQ6, and BRIQ7 did not tolerate water and absorbed a significant amount of water, leading to the samples crumbling and disintegrating

to some extent. They produced more fines when preparing them for testing. Alternatively, BRIQ7 sample was cut dry without the use of water, which resulted in the cube sample not having smooth edges. BRIQ6 could not be cut dry, as it disintegrated under the cutting force. However, an irregular piece of the briquette was used for testing.

An average of 3 briquettes measurements was used to determine each briquette's recipe apparent density based on their mass and geometry (Assuming a perfect cylinder). True density of briquettes was determined using gas pycnometer AccuPyc II 1340. Helium was used as displacement gas in the pycnometer, purge fill pressure and cycle fill pressure were set to 134.45 kPa. Briquette's porosity (ε) was then calculated as follows:

$$\varepsilon = \frac{\rho_S - \rho_a}{\rho_S} \times 100, \qquad (1)$$

Where ε is the briquettes porosity, ρ_S is the density determine by pycnometer in g cm^{-3} and ρ_a is the apparent density determined based on briquettes mass and dimensions in g cm^{-3}.

Table 9 shows the average of briquettes' height, apparent density, true density and porosity.

Table 9 Apparent density of produced briquettes.

Briquette	Height (cm)	Apparent density (g cm^{-3})	True density (g cm^{-3})	Porosity (%)
BRIQ1	40.60	2.23	3.0827	27.77
BRIQ2	39.28	1.49	2.3990	37.87
BRIQ3	33.60	2.24	3.2139	30.27
BRIQ4	45.42	2.14	3.1223	31.41
BRIQ5	27.58	1.62	2.7809	41.71
BRIQ6	44.17	2.33	2.9307	20.55
BRIQ7	34.08	1.88	2.8929	35.07

Decreasing the porosity of the agglomerate has a positive influence on the final strength as the agglomerate density increase with the decreased porosity which ultimately results in an increase in agglomerates strength.[51]

3.3. Methods

Methods used to assess the behavior of the briquettes in an EAF are presented below.

3.3.1. Cold compression strength

Cold compression strength (CCS) is generally used to assess the briquette ability to withstand storage, handling and charging in a bucket. CCS test has been carried out using an INSTRON multifunctional breaking strength-testing machine with a 500 kN load cell. Samples had been placed in between the load cell (upper position) and the moving bar (lower position). The moving bar subsequently had been driven up just before the sample touched the load cell. Thus, testing procedure started basically

following ISO BS 4700:2015 with a moving speed of the lower bar of 15 mm/min. Test has been aborted manually when maximum resistance reached or visual disintegration of the sample itself noticeably started. CCS test for BRIQ4 was carried out using the same standard but employed a 100 kN Zwick/ Z100 testing machine. The test was considered completed either when the load fails to less than 50% of the maximum load recorded or when the gap between the platens decrease to less than 50% of the initial heigh of tested briquette. Maximum load was recorded, and compression strength was obtained according to:

$$\sigma_c = \frac{F}{A}, \qquad (2)$$

Where σ_c is compression strength in MPa, F is the recorded force in N and A is the cross-section area of tested briquette in mm^2.

To define a threshold value for the tailor-made briquettes, samples of ferroalloy (FA) and lime (used in EAF steel plant No.3) were also tested in the same conditions as briquettes. However, due to the irregular surface and sizes of such raw materials, the CCS was expressed as the maximum load registered before load drop.

3.3.2. Drop damage resistance

The drop test is a good qualitative analysis to provide a parameter for the loading and unloading of briquettes inside a cargo vehicle or the briquettes loading inside a furnace. Drop test was performed to assess drop damage resistance after long curing time (2 years) by dropping one briquette per time from a height of 2 meters onto a steel plate. Residual briquette mass was recorded every 5 drops and the test was considered completed either when the briquette lost 50% of its mass or after it has survived 50 drops. 2-3 briquettes per each recipe were tested. Retained mass reported is the average mass of samples tested of each recipe. In addition, to test early development of drop damage resistance, simulating short curing and storage time of briquettes, BRIQ4 was dropped from a heigh of 1 meter after curing for 2 days, and a height of 5 meters after curing for 7 days. To define a threshold value of drop damage resistance for the tailor-made briquettes, samples of ferroalloys that are used in plant 3 EAF were also tested in the same conditions as described.

3.3.3. Optical dilatometry

Dilatometry testing was conducted in a horizontal tube furnace with a computer-connected camera. Cubic samples used in dilatometer tests were roughly 1 cm^3 cubes cut from the same position of tested briquettes. In dilatometer testing, the cubic sample was heated at a rate of 5 °C min^{-1} in flowing nitrogen gas at a rate of 3 l min^{-1}. The computer-connected camera was set to save the sample image at 5 °C intervals. Dilatometer used is a homemade apparatus, assembled at process metallurgy research unit at the University of Oulu. Figure 4 shows a schematic of the apparatus used to better clarify the testing setting.

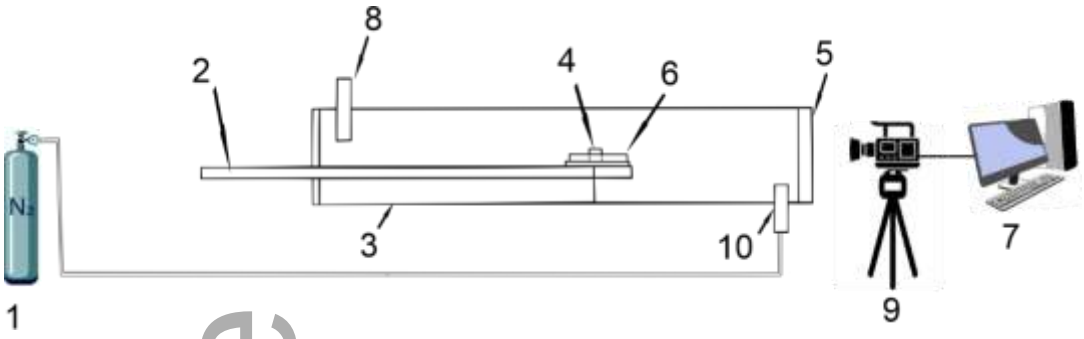

Figure 4 Dilatometer apparatus used in the tests. 1. Nitrogen gas cylinder 2. Push rod with thermocouple 3. Water-cooled stainless steel tube furnace 4. Sample 5. Quartz glass 6. Sample holder 7. Computer system 8. Gas outlet 9. Camera 10. Gas inlet.

Since the samples used were relatively large, a special sample holder was required. The sample holder had to contain the sample without obstructing the view of the camera so that it could capture the briquettes' full border from bottom to top. A longer mold was 3-D-printed with edges only on the sides so that it would not obstruct the camera view. The mold was used to produce the sample holders employed in the tests. An example of sample mounted on the sample holder before and after dilatometry testing is shown in Figure 5.

(a) (b)

Figure 5: Cubic 1 cm^3 sample cut from BRIQ3 mounted on a sample holder before (a) and after (b) dilatometry testing.

3.3.4. Briquette melting trial

A chamber furnace was used to conduct melting trials. Industrial EAF slag samples were obtained from two different operating plants, plant No.1 and No.2. Slag was ground and analyzed for chemical composition using XRF. The chemical compositions of both types of slag used are presented in Table 10.

Table 10: Chemical composition of plant No.1 and plant No.2 slag (wt.-%), determined through XRF.

	Na_2O	MgO	Al_2O_3	SiO_2	SO_3	K_2O	CaO	Cr_2O_3	MnO	Fe_2O_3
Plant 1 slag	0.21	5.70	14.58	14.9	0.17	0.02	22.18	2.57	4.33	29.41
Plant 2 slag	0.53	3.36	5.93	29.17	0.31	0.05	15.49	1.85	3.49	27.36

The industrial slag samples were then prepared for the trial by grinding and roasting them for four hours at 1300 °C to ensure there was no metallic iron that could dissolve the platinum crucible. Then, 40 g of slag was placed in the platinum crucible. BRIQ6 was tested with molten slag from plant No.1, while BRIQ7 was tested with slag from plant No.2. In each trial, slag was placed in a platinum crucible and inserted into a chamber furnace heated to 1550 °C. When the slag became liquid, the door of the furnace was opened, and a 2 g sample was cut from the briquette and then placed in the crucible, on the top of the melt. A camera was placed in front of the chamber furnace so that when the furnace door was opened, the camera would capture the slag surface and sample on top. The door was open for less than 5 seconds to avoid significantly cooling the furnace.

3.3.5. TGA-MS tests

Thermogravimetry is a method in which, mass change of a sample is measured against temperature change through a thermobalance. Thermogravimetry can be used to assess the thermal stability of material as function of time or temperature. a derivative thermogravimetry (DTG) curve is the plot of dm/dT against temperature and is used to determine the temperature at which the mass loss was at maximum.[52] Mass Spectrometry is used to analyze the evolved gases during thermal analysis. It is a very sensitive instrument that can detect gases with concentrations as low as 8 ppb. MS usually employs He as a carrier gas. Part of the gases leaving the TG device is routed to MS instrument through a heated ceramic capillary. In MS ionization chamber, the gases are bombarded by electrons, and gas molecules are fragmented into positive ions which are separated according to the ration of their mass/charge. The intensity could then be plotted against mass/charge ratio based on the ion current measurement.[53]

To perform TGA-DTG-MS testing, 1 cm^3 cubic sample cut from BRIQ4 was used. Testing was carried out using an STA 449F3 Jupiter thermal analyzer coupled with a mass spectrometer and a NETZSCH QMS 403 to analyze the evolving gases. The heating rate was 5 °C/min in Argon gas with a flow rate of 60.0 ml/min, up to a final temperature of 1300 °C. TGA-DTG-MS analysis was conducted using NETZSCH Proteus® software. The 3-D MS curves generated were assessed for any indications of unwanted emissions.

3.3.6. Full briquette reduction trials

Full briquette reduction was investigated using a tube furnace. The tube furnace employed was previously used in reduction experiments.[54] The furnace and its components are presented in Figure

6. It had a 95 mm inner diameter and utilized a pre-determined program with varying gas compositions and temperatures during testing. This made it possible to perform both isothermal and dynamic tests. The setup was capable of carrying out tests at temperature up to 1100 °C. The test samples' mass was continuously measured through a scale to which, the sample basket was connected.

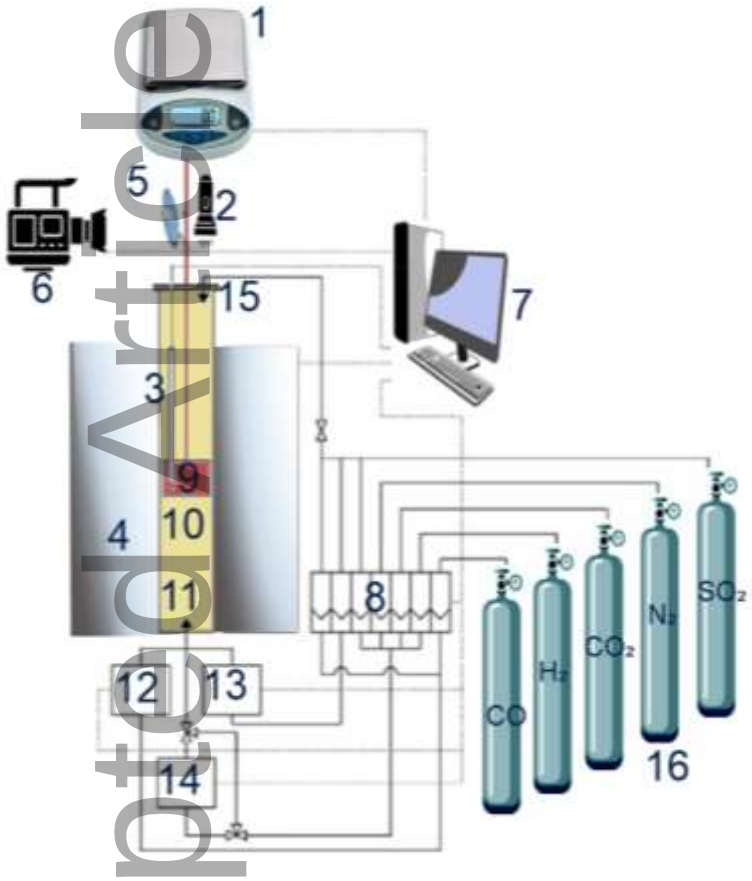

Figure 6: Schematic diagram of the experimental furnace setup with a (1) scale, (2) light torch, (3) thermocouple, (4) electrically heated furnace, (5) mirror, (6) video camera, (7) computer system, (8) mass flow control, (9) sample basket, (10) reduction tube, (11) water pump, (12) sulfur generator, (13) potassium generator, (14) gas inlet, and (15) transparent lid and cooling gas inlet, as well as (16) gas cylinders.

In each reduction test, a full briquette of each recipe was placed in the basket, which was then lowered into the furnace. A nitrogen flow at 10 l/min was maintained for 5 min at room temperature to purge the furnace. The reduction pre-determined program was initiated to simulate EAF conditions. Reducing gases were introduced into the furnace according to the reduction program shown in Table 11, while simultaneously heating the sample from room temperature to 1100 °C.

Table 11: Gas composition during dynamic reduction in the reduction tube furnace.

Gas	N_2	CO	CO_2	H_2

(%)	31.00	50.00	15.00	4.00

The gas flow was maintained at 15 l/min until the target temperature was reached. The samples were then allowed to cool in nitrogen flowing at a rate of 10 l/min to avoid re-oxidizing the samples.

4. Results and Discussion

4.1. Cold compression tests

The results of cold compression test are shown in Figure 7, showing the final compression strength with production load variation from 10 to 40 MPa. As reported in Figure 7, the cold compressive strength of all the investigated briquettes generally increased by increasing the pressure manufacturing process. Previous researchers concluded that for certain briquettes recipes, increasing manufacturing pressure would always result in an increase in the briquette strength.[20] However, BRIQ1 and BRIQ3 experienced a slight decrease in cold compression strength when increasing manufacturing pressure to 40 MPa. This observation is in agreement with other researchers who concluded that an increase in manufacturing pressure may result in an decrease in drop damage resistance[17] and final strength[50]. The reason is that friable material might crack under the excessive pressure. All the briquettes were tested after 10 days of curing, except for BRIQ4 which was investigated also after 2 and 7 days of curing. In particular, BRIQ4's strength was more than 17 MPa after 2 days of curing and increased to 22 MPa after 7 days of curing. BRIQ1 and BRIQ3 were able to withstand a stress of more than 50 MPa after 10 days of curing and were deemed to have suitable mechanical characteristics. The scarcest compression resistance was exhibited by BRIQ2 and BRIQ5 which hardly overcame 20 MPa of CCS when manufactured at 40 MPa. However, all the tested recipes had a minimum CCS largely higher than the compressive resistance of reference materials, i.e., ferroalloys (FA) and lime lumps. In detail, being the ferroalloys and lime lumps irregular, the maximum breakage strength was expressed in term of force, that reached 1074.2±315.3 and 403.5±99.8 daN, respectively. By converting the briquettes CCS in force, according to briquettes diameter, BRIQ2 and BRIQ5 resistance at the minimum manufacturing pressure was three times higher than the value of ferroalloys lumps. Thus, from cold compression strength point of view, all the manufactured briquettes were judged suitable to be charged in the scrap bucket because they can withstand the scraps pressure.

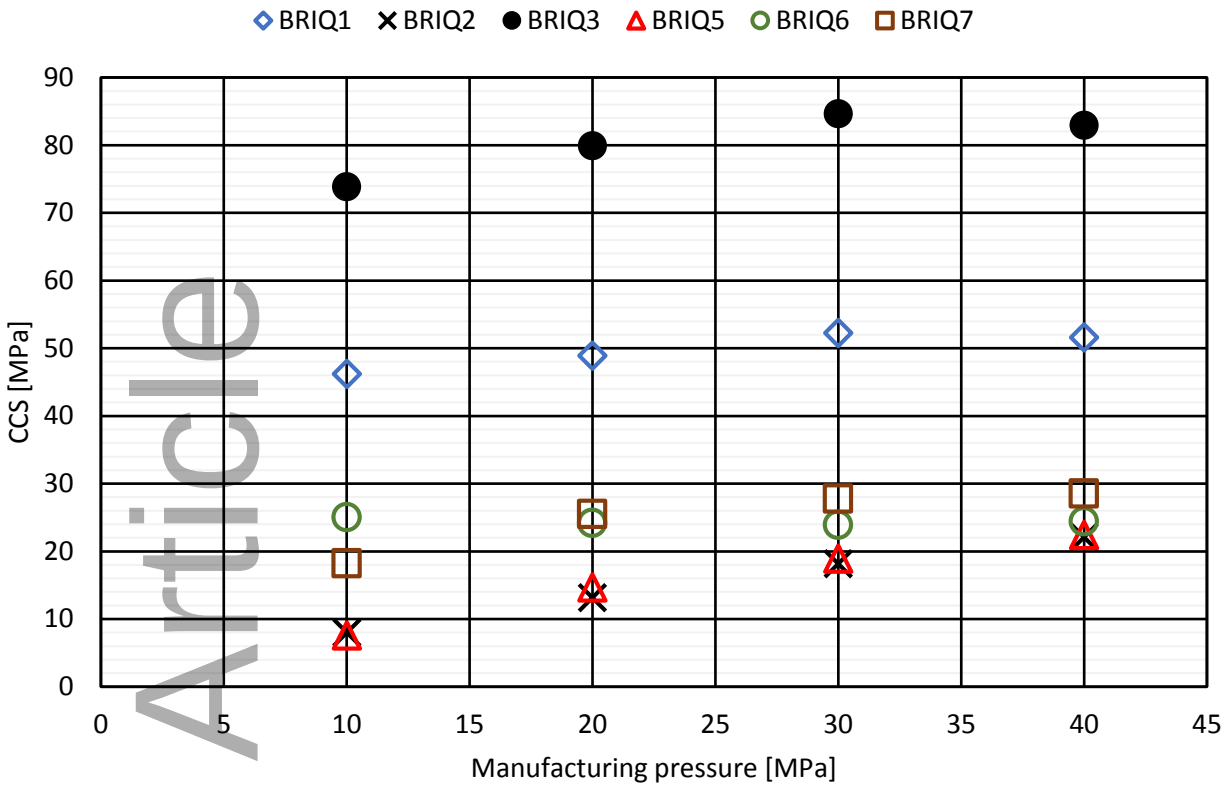

Figure 7 CCS values as a function of manufacturing pressure for different briquettes investigated

4.2. Drop tests

To test early drop damage resistance, BRIQ4 was dropped from a height of 1 m after curing for 2 days and a height of 5 m after curing for 7 days to test early drop damage resistance of the briquette. Testing procedures were considered completed after 50 drops or when the briquette's mass fell below 50% of its initial mass. The briquette was able to withstand 50 drops before falling below 50% of its initial mass in both tests. All the briquettes were also tested for their long term drop damage resistance after more than 2 years of curing. 2-3 briquettes were tested per recipe, and their drop damage resistance is shown in Figure 8. At least 2 briquettes tested from recipes of BRIQ 1, 3, 4, 6 and 7 were able to withstand 50 drops without losing more than 50% of its mass. BRIQ2 and BRIQ5 showed poor drop damage resistance and none of the tested briquettes survived more than 10 drops.

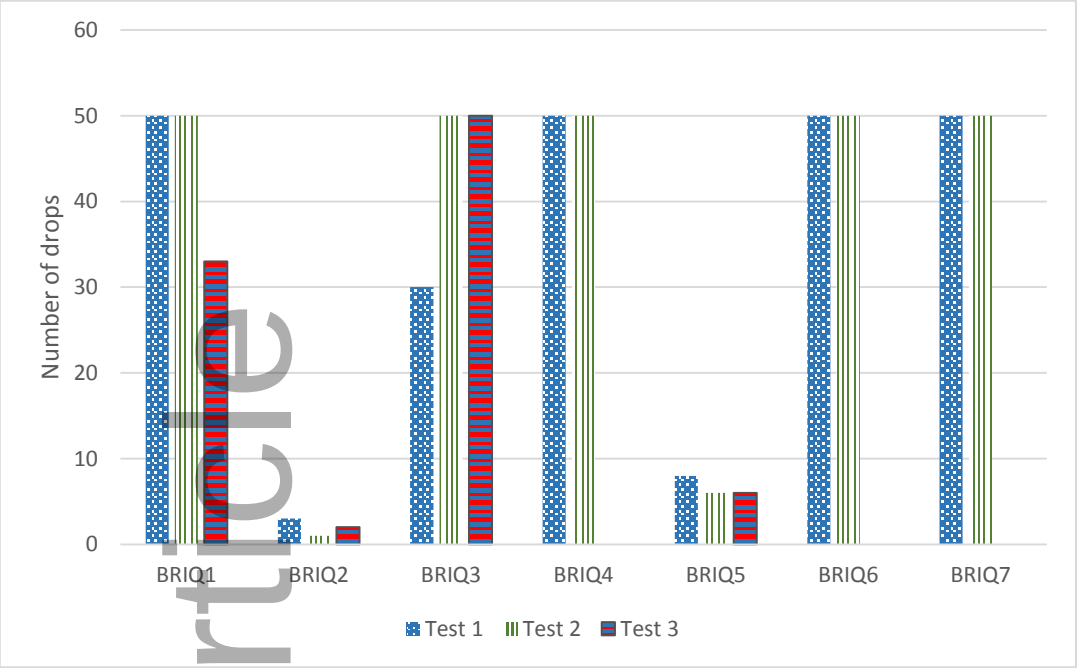

Figure 8 Number of drops of each briquette before reaching 50 drops or losing 50% of its initial mass

Figure 9 shows drop test results of produced briquettes showing number of drops and residual mass retained after every 5 drops. BRIQ1 and BRIQ3 show similar results. Although one of the briquettes of each recipe failed before surviving the 50 drops, the average of mass retained is higher than 65% in both briquettes, which was considered acceptable from operational point of view. An outstanding behavior was observed for BRIQ 4, 6 and 7. Not only all tested briquettes survived 50 drops, but also the three recipes composition had the lowest mass detachment, which was on the same level as Ferro alloys used in EAF steel plant No.3 which was used as a reference material in this work. The only two recipes that did not survive 50 drops and had very poor performance compared to reference material (Ferroalloy stones) were BRIQ2 and BRIQ5 that literally disintegrated after few drops with the highest drop damage resistant briquette surviving 3 and 8 drops, respectively before falling below 50% of its initial mass. Regarding BRIQ2 poor performance, it was likely due to some internal pressure developed by CaO hydration that contrasted the binding effect of starch. For instance, BRIQ2 was made mainly by belt conveyor fines, which mostly consisted of lime fines. CaO can slowly react with atmospheric moisture and transform into portlandite ($Ca(OH)_2$). Since the volume of the briquette is constrained, the volume expansion due to lime hydration rises the stress within the briquette, which collapse soon when stressed. BRIQ5 did not appear to have an optimum mechanical performance, as indicated by CCS test. Porosity of briquettes appear to have a role in the mechanical properties of briquettes with BRIQ5 and BRIQ2 having the highest porosity at 41.71 and 37.87%, respectively.

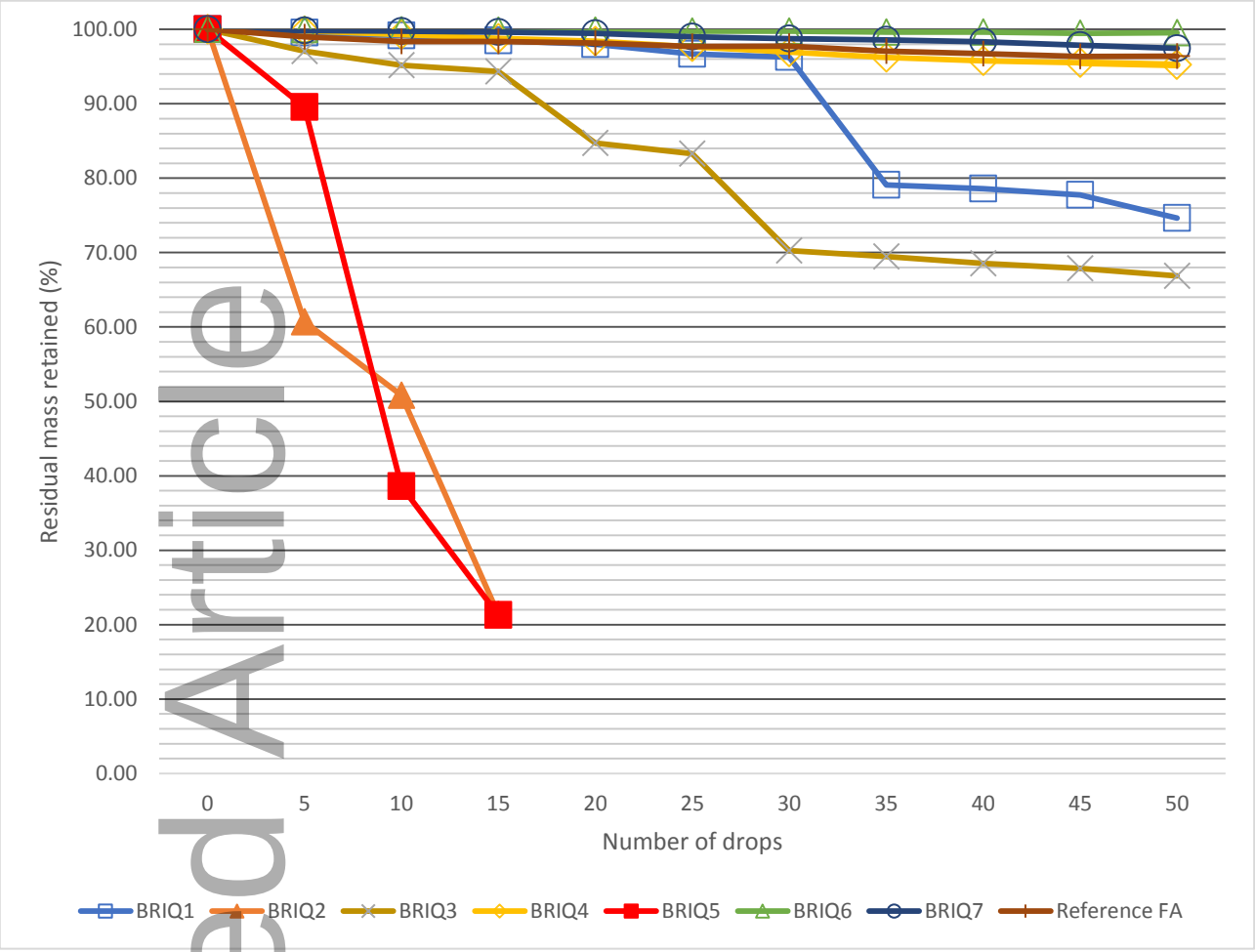

Figure 9 Drop test results of produced briquettes showing number of drops and residual mass retained after every 5 drops.

4.3. Optical dilatometry

Optical dilatometry trials were performed to investigate the softening and melting behavior of selected briquettes. The tapping temperature in industrial EAFs is typically in the range of 1580–1680 °C. Therefore, it is important to ensure the melting of added charge at the intended temperature to avoid tap-hole clogging problems.[40] Figure 10 and Figure 11 show the temperatures at which major changes took place for each test briquette. Stages of the briquettes' melting included shrinkage, where the briquettes retained their shape without significant deformation. In the softening stage, the briquettes' shape started to deform. In the melting stage, surface bubbling was observed, and the specimens started to collapse under their own weight.

BRIQ	Start	Shrinkage	Softening	Melting	End
1	50 °C	1210 °C	1300 °C	1330 °C	1460 °C
	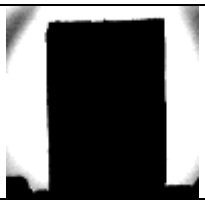	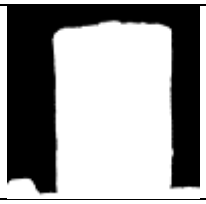	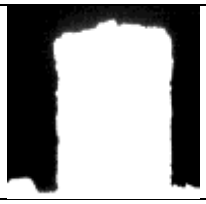	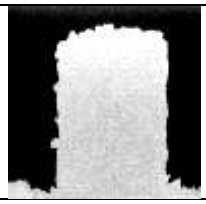	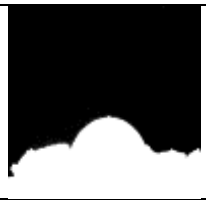
2	50 °C	1420 °C	1450 °C	1495 °C	1510 °C
	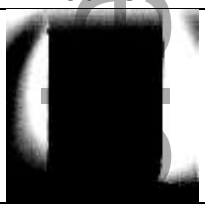	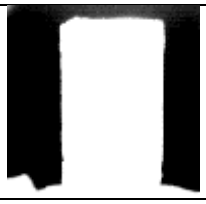	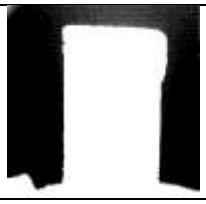	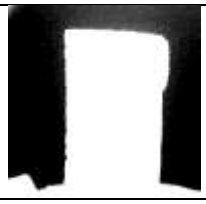	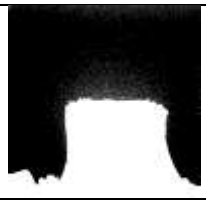
3	50 °C	825 °C	1045 °C	1375 °C	1500 °C
		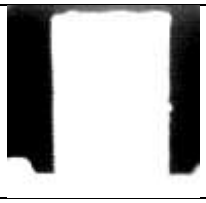	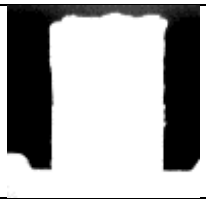	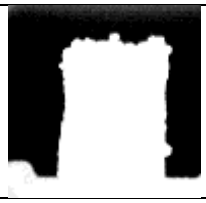	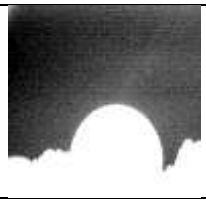
4	50 °C	995 °C	1335 °C	1370 °C	1500 °C
	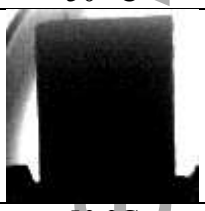	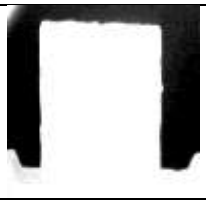	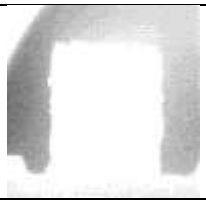	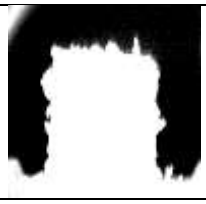	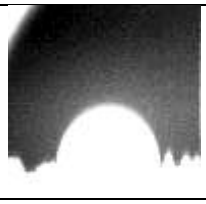
6	50 °C	1380 °C	1385 °C	1395 °C	1500 °C
		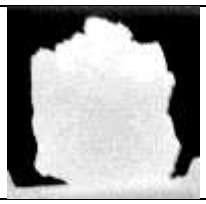	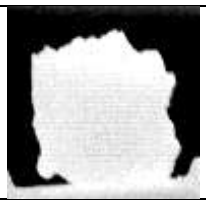	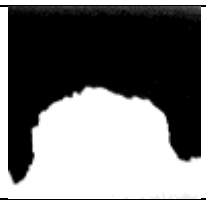	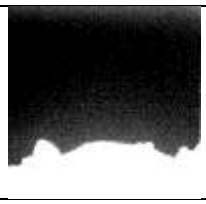
7	50 °C	1340 °C	1380 °C	1395 °C	1465 °C
	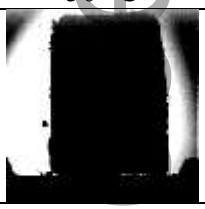	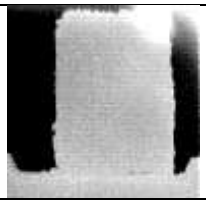	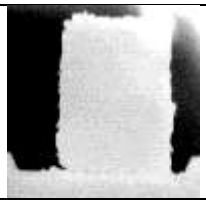	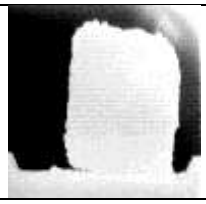	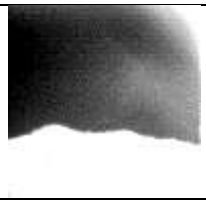

Figure 10: Selected dilatometry pictures of different briquettes.

BRIQ6 did not seem to exhibit significant shrinkage up to 1385°C. Beyond 1385°C, the briquette proceeded to melt rapidly. Similar observation was made when testing BRIQ7. On the other hand, BRIQ5 appeared to disintegrate at low temperatures, as shown in Figure 11. The poor behavior of BRIQ5 indicate that it would be inadequate for use in EAF as the briquette would be prone to disintegration at low temperature, resulting in fines generation and loss of material, eventually leading to lower productivity.

BRIQ5	50 °C	180 °C	225 °C	785 °C	1500 °C
					

Figure 11: Selected dilatometry pictures of BRIQ5 show how it disintegrated at very low temperatures.

Briquettes containing the highest iron oxide and carbon content exhibited the highest degree of shrinkage during the heating process, which was presumed to be linked to oxide reduction. It could be observed that the shrinkage of BRIQ3 and BRIQ4 was higher than that of BRIQ1. The self-reducing briquettes started to melt in temperatures over 1300 °C. After the test, the self-reducing capability of samples was confirmed. Information regarding the order at which briquettes melt would be beneficial to operation of EAF in order to have better control over the process. Choice of briquettes used in EAF may lead to lowering tapping temperature and subsequently increase productivity.

The slag former briquettes, BRIQ6 and BRIQ7 started to show signs of shrinkage near 1400 °C. BRIQ6 was fully molten by 1400 °C and BRIQ7 by 1465 °C. This indicates that these briquettes would melt sooner than scrap and contribute to slag formation. High CaO-bearing BRQ2 melted at the 1498 °C, which means that it could contribute to the basicity of slag in later slag formation phases.

Since most of the self-reducing briquettes' mass solidified into a metallic drop as shown in Figure 5 and Figure 10, the microstructure and chemical composition of them were investigated through SEM-EDS and optical microscopy. The chemical composition was typical of cast-iron, as shown in Table 12. BRIQ1 had a pearlitic matrix surrounded by primary cementite and graphite flakes, while BRIQ3 and BRIQ4 had a pearlitic matrix surrounded by primary cementite plaquettes, as shown in Figure 12.

Table 12: SEM-EDS analysis of the reduced briquettes after dilatometer testing.

wt.-%	C	F	Al	Si	S	Cr	Mn	Fe
BRIQ1	6.2	-	0.2	0.2	0.1	0.8	0.6	92.0
BRIQ3	3.0	0.9	-	0.5	0.4	1.3	0.6	93.4
BRIQ4	2.9	-	0.2	0.2	0.2	1.0	-	95.6

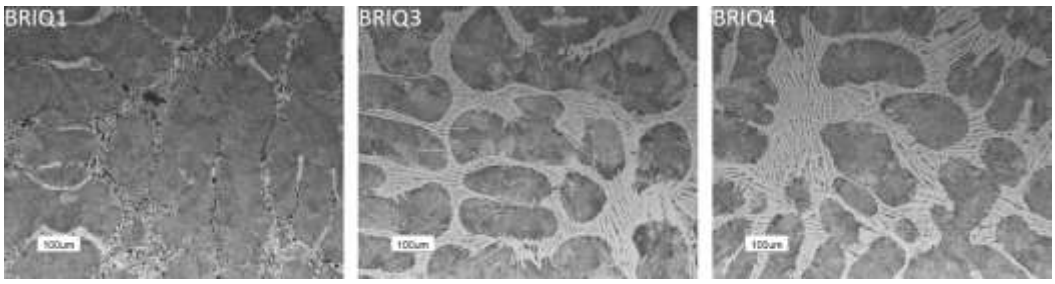

Figure 12: Microstructure of reduced briquettes by optical microscope. Etching: Nital 2%. Primary cementite (white), perlite (grey), and graphite (black).

Residual unreduced material from BRIQ1 and BRIQ4 were also analyzed by XRD, and the results are shown in Figure 13. The former was composed of unreduced iron oxides, mainly wustite, and residual carbon (note the huge and wide peak at 25° 2Θ). The presence of Al-Ca-Si-Mg compounds was probably due to the reaction between unreducible oxides within the briquettes and the Al_2O_3 plate of dilatometer. The latter showed a considerably lower residual amount of carbon and iron oxides, but no residues were found in the crucible for BRIQ3. This means that the whole briquette mass reduced to iron and confirms that the self-reducing capacity of BRIQ3 was better than that of BRIQ1.

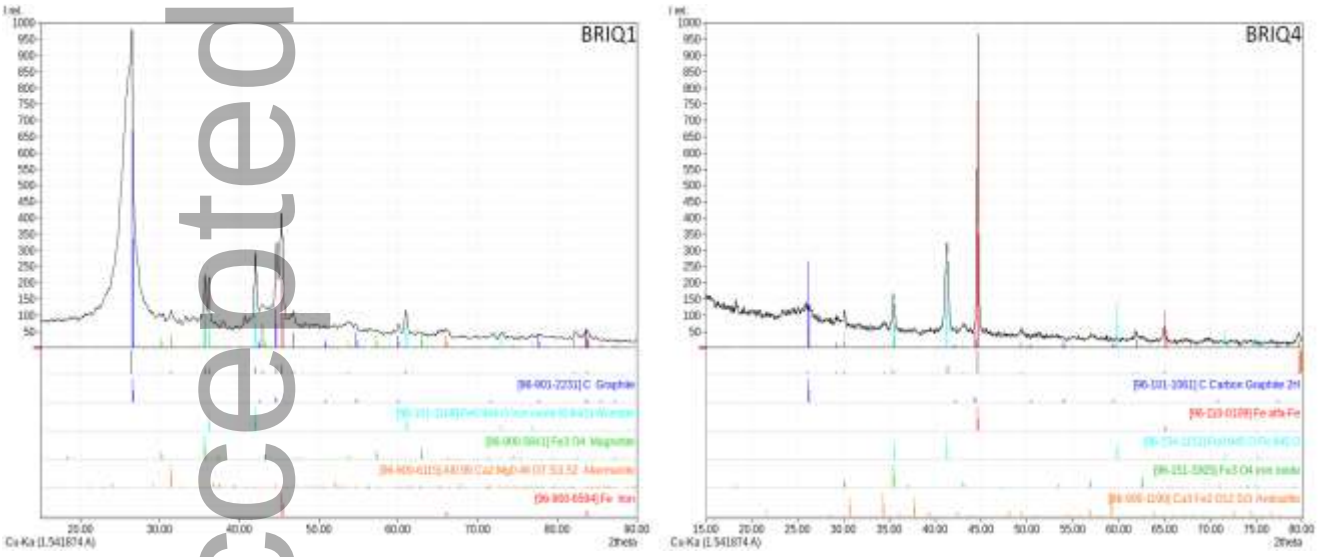

Figure 13: XRD patterns of residual materials collected from the sample holder after dilatometer testing of BRIQ1 and BRIQ4.

In conclusion, from the optical dilatometry trials, we can conclude that BRIQs 1, 2, 3, 4, 6, and 7 are suitable for use in EAF from a melting perspective, while the use of BRIQ5 would be challenging due to cracks occurring at temperatures over 180 °C. The hydrophilic behavior of BRIQs 5, 6, and 7 encountered during sample preparation suggests that these briquettes would not withstand high humidity during storage, which may limit their use.

4.4. Melting trials

In the first melting trial, slag from plant 1 was melted in a muffle furnace, and an approximately 1 cm^3 piece cut from BRIQ6 was placed on top of the slag. In the second trial, a BRIQ7 piece was used with slag from plant 2. Figure 14 shows the BRIQ6 sample's melting stages when placed in the slag. The BRIQ6 piece ignited immediately after being placed on top of the molten slag. A flame appeared on the surface of the sample 15 sec after placing the sample on top of the slag, with no black smoke detected. No flames or black smoke was detected 28 sec after the sample was placed on top of the slag, and the sample appeared to start melting. The sample could still be detected with some bubbling around it within 44 sec after placing the sample on top of the slag. Within 55 sec after placing the sample on top of the slag, traces of the sample could still be detected, with more intense bubbling surrounding the remains. The sample appeared to have completely melted 67 sec after placing the sample on top of the slag. No bubbling was detected on the surface of the slag, and no flames or black smoke was detected. By 90 seconds, the briquette had completely vanished, and only some bubbling of the slag was observed. After the sample completely vanished, the crucible was tapped, and the slag was allowed cool in the ambient atmosphere. Similar behavior was observed for BRIQ7, as shown in Figure 15.

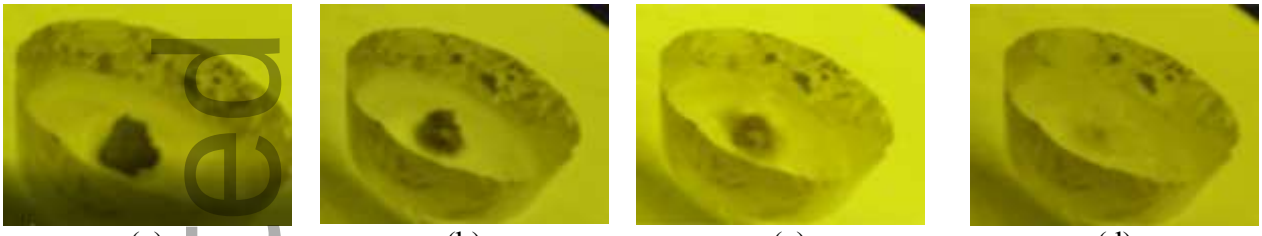

(a) (b) (c) (d)

Figure 14 BRIQ6 briquette directly after placing it on top of plant 1 molten slag (a), after 15 seconds (b), after 25 seconds (c), and after 55 seconds (d).

(a) (b) (c) (d)

Figure 15 BRIQ7 briquette directly after placing it on top of plant 2 molten slag (a), after 20 seconds (b), after 30 seconds (c) and after 55 seconds (d).

The chemical compositions of plant 1 and plant 2 slags were determined using XRF prior to and after the melting trial. From a chemical viewpoint, a slight increase in CaO and SiO_2 was observed after

the briquettes' dissolution, while the other compounds remained relatively unchanged, as shown in Table 13.

Table 13: Chemical composition (wt.-%) of industrial slags prior to and after the melting trial.

wt.-%	Na_2O	MgO	Al_2O_3	SiO_2	P_2O_5	SO_3	CaO	TiO_2	Cr_2O_3	MnO	Fe_2O_3
Before briquette melting											
Plant 1 slag	0.21	5.70	14.58	14.94	0.46	0.17	22.18	0.51	2.57	4.33	29.41
Plant 2 slag	0.53	3.36	5.93	29.17	0.23	0.31	15.49	0.45	1.85	3.49	27.36
After briquette melting											
Plant 1 slag	0.31	3.93	10.66	16.63	0.45	0.02	25.55	0.52	0.86	3.50	30.83
Plant 2 slag	0.48	4.62	6.84	30.60	0.24	0.12	18.18	0.47	1.23	3.18	26.07

4.5. TGA-DTG-MS

Figure 16 shows TGA-DTG-MS curves for BRIQ4. DTG peaks in combination with MS indicate which reactions take place at different stages of heating. BRIQ4 mostly consisted of grinding sludge, oxi-cutting fines and coal injection with starch and paper fibres used as part of the binding system. Griding sludge main constitute was metallic iron, while oxi-cutting fines mainly consisted of magnetite.

Mass loss between 0 and 185°C amounts to 4.62%. The DTG peak at 141.80°C indicates water evaporation supported by the formed peak of H_2O, which has a mass-to-charge ratio (m/z) of 18 in MS and originated mainly from grinding sludge and to a lesser extent from other briquettes constitutes. Small peak of CO_2 around the same temperature indicates the degradation of paper fibres which contributed to 1.9% of briquettes mass.

Mass loss between 185 and 316°C amounts to 7.90%. A DTG peak appears at 271.80°C accompanied by H_2O ((m/z=18), CO (m/z=28) and CO_2 (m/z=44) MS peaks indicating the degradation of starch used as a binder. Starch itself is reported to degrade in 3 stages.[55] In the first stage water is evaporated up to 120°C. The main degradation of starch takes place in the second stage, which occurs up to 350°C, and in which pyrolysis is accompanied with release of water, carbon dioxide, carbon monoxide and methane. The third stage ends around 600°C with the formation of carbon black. Carbon black may contribute to the reduction of iron oxides within the briquette at higher temperature.

There are two stages of devolatilization of coke, the first one being between 300 and 600°C, and the second ne above 600°C.[56] Mass loss between 316 and 450°C amounts to 3.59% with a small DTG curve peak at 336°C which is likely due to the release of chemically bound water, and due to the first

stage of coke devolatilization. MS peak H_2O (m/z=18) indicates that chemically bound water release takes place up to a temperature of 450°C.

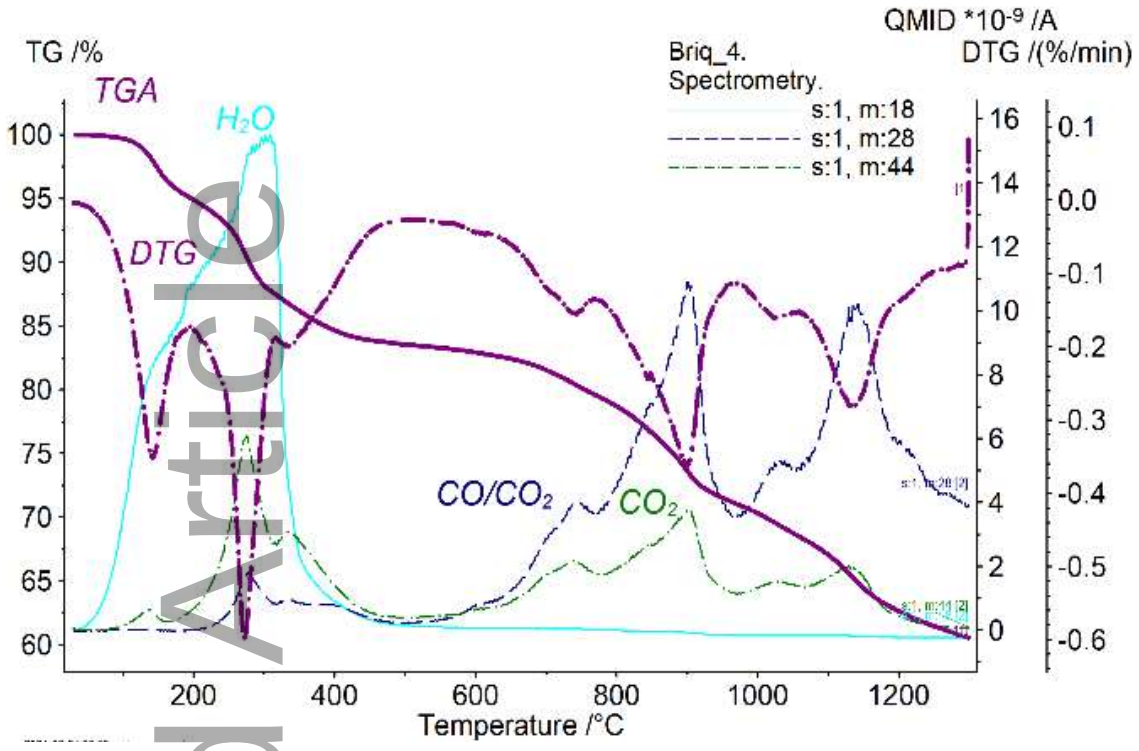

Figure 16: TGA-DTG-MS of BRIQ4 showing evolving gases at different stages of heating.

Hydrogen and carbon monoxide are generated during pyrolysis of coal which contribute to reduction of iron oxides in stepwise as follows:

$3Fe_2O_3 + H_2/CO = 2Fe_3O_4 + H_2O/ CO_2$ (2)

$Fe_3O_4 + H_2/CO = 3FeO + H_2O/ CO_2$ (3)

$FeO + H_2/CO = Fe + H_2O/ CO_2$ (4)

Carbon gasification takes place through reacting with carbon dioxide, resulting from reduction process and steam according to the reactions:

$CO_2 + C = 2CO$ (5)

$H_2O + C = CO + H_2$ (6)

Product hydrogen and carbon monoxide contribute to the reduction of iron oxides in cyclic reactions provided there is enough carbon. Complete reduction of hematite-coal mixture to metallic iron takes place at lower temperature when compared to magnetite-coal mixture.[57] The presence of different iron oxides in mixture with coal might be the reason why a reduction step gives two DTG peaks as shown in Table 14 which contains mass loss over temperature range and corresponding DTG peaks.

Although methane, and water have smaller intensity peaks, they could be detected in the range between 500 and 1300°C. Methane (m/z=16) is one of the products of coal pyrolysis, and it contributes to the iron oxide reduction. It could also be formed through secondary reactions with the catalytic effect of formed metallic iron as follows[56]:

$C + 2H_2 = CH_4$ (7)

$CO + 3H_2 = CH_4 + H_2O$ (8)

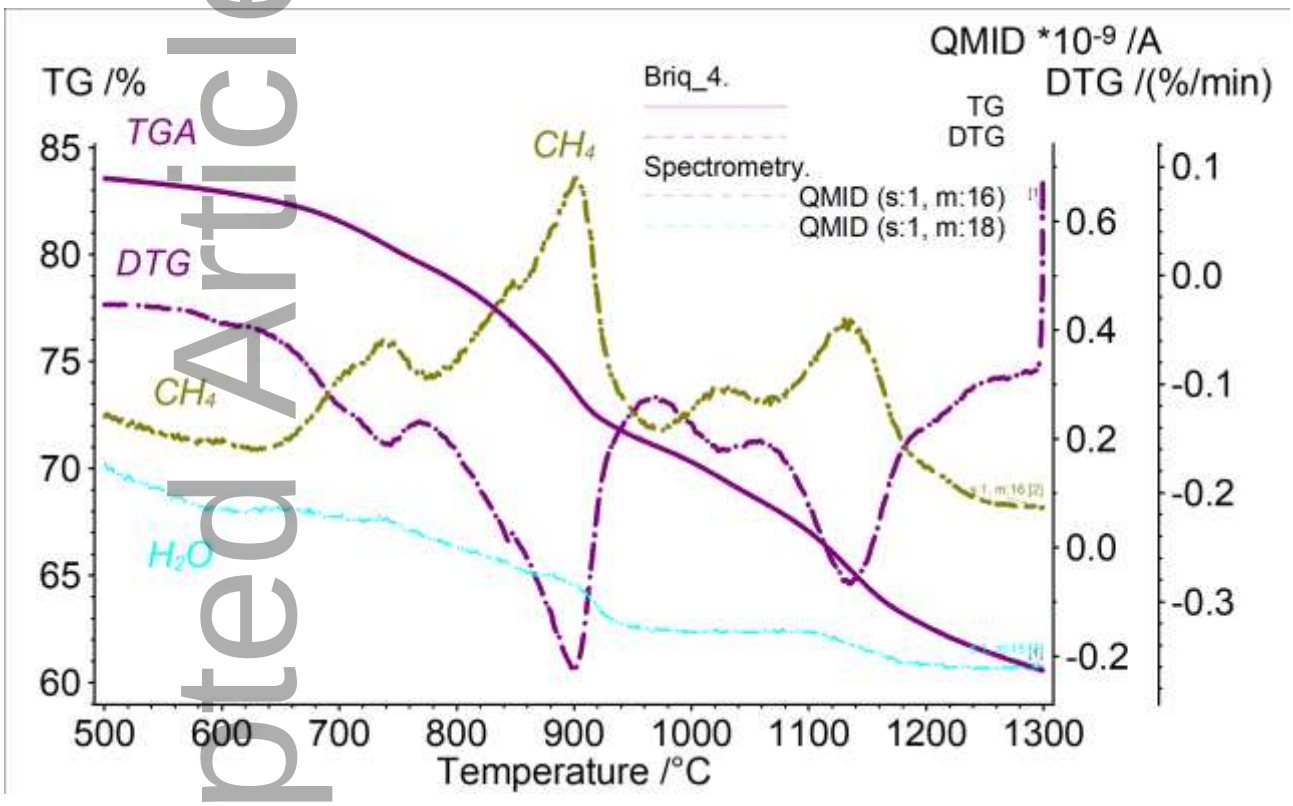

Figure 17 TGA-MS in the temperature range between 500-1300°C showing H_2O and CH_4 peaks

Table 14 TGA-MS BRIQ4 mass loss and reactions up to 1300°C

Temperature (°C)	Mass loss (%)	DTG peak (°C)	Main reaction
0-185	4.62	141.80	Absorbed moisture evaporation and decomposition of paper fibres
185-316	7.90	271.80	Main stage decomposition of starch
316-450	3.59	336.00	Chemically bound water is released First stage of coal devolatilization
450-550	0.60%		Third stage of decomposition of starch
550-775	3.84	743.00	Second stage of carbon devolatilization $Fe_3O_4 + H_2/CO = 3FeO + H_2O/ CO_2$
775-975	8.50	899.80	
975-1060	2.49	1023.00	Coke gasification $CO_2 + C = 2CO$ $FeO + CO = Fe + CO_2$
1060-1300	7.89	1135.20	

To examine the presence of unwanted gas products, 3-D mass spectrometry was used to detect abnormalities that may indicate the presence of unwanted evolved gases, such as heavy hydrocarbons. As shown in the 3-D spectra presented in Figure 18, high peaks are found at m/z of 20 and 40, which correspond to purging the argon gas used in the test. The MS peaks at m/z if 18, 28 and 44 correspond to H_2O, CO, and CO_2, respectively. However, no heavy evolved gases are indicated by a higher m/z number, as there were no peaks detected in the m/z range between 50 and 100.

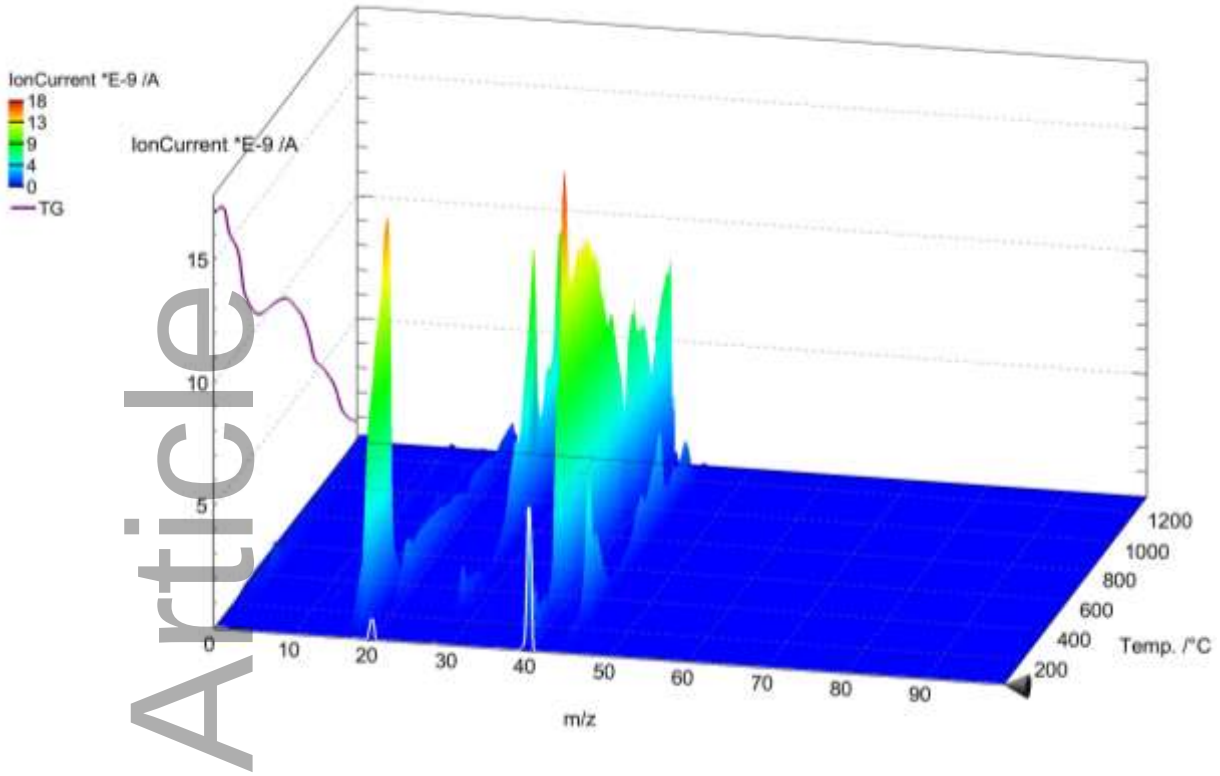

Figure 18: Mass spectrometry of briquette BRIQ4 showing evolving gases with an m/z range up to 100.

4.6. Full briquette reduction

4.6.1. Briquette reduction behavior

Figure 19 shows the mass loss of fully intact BRIQs 1, 3, and 5 during reduction, as well as the mass loss of BRIQ4 cut into four smaller pieces (each is 1/8 of full briquette size). During the testing of BRIQ1, off-gas fumes were extremely thick and ignited upon exiting the furnace. To protect the measurement equipment, the trials had to be aborted after 20 min. Unlike BRIQ1, BRIQ3 did not show excessive fuming. The briquette stayed intact during heating as only some cracks were generated. The weight reduction was, at the maximum temperature, approximately 23 wt.-%. It differs from TGA-MS is that in the furnace, heating is much faster and the sample size smaller; the furnace trial took approximately 35 min, while TGA-MS took longer than 5 h. This suggests that the higher reducing atmosphere in the furnace and the slower heating time and smaller sample in TGA-MS compensated each other. BRIQ5 behaved very similar to BRIQ3. Mass reduction was only a few percentage points smaller than for BRIQ3.

To examine how homogenous the briquettes were, four of the briquettes made based on the BRIQ4 recipe were cut and reduced in the same run. The cutting was performed so that each briquette was cut into a lower and upper part. Then, the upper part of each briquette was again cut into four quarters, which results in a single piece being 1/8 in size of full briquette. Figure 20 shows the briquette pieces

before and after the reduction experiment. After mass measurements were taken during the post reduction experiments, it was clear that each briquette piece from the four different briquettes exhibited the same mass loss, indicating that the briquettes were homogenous. BRIQ4 exhibited around 30% mass loss during heating which is line with TGA-MS measurements. Although BRIQ3 has very similar composition to BRIQ4, the mass loss rate in BRIQ3 was much slowed when compared to BRIQ4. The reason is likely that heat transfer was much easier with smaller cut samples in BRIQ4 with higher surface area. This result imply that briquette size plays a major role in reduction, and with smaller briquette size, reduction could be achieved at higher rate.

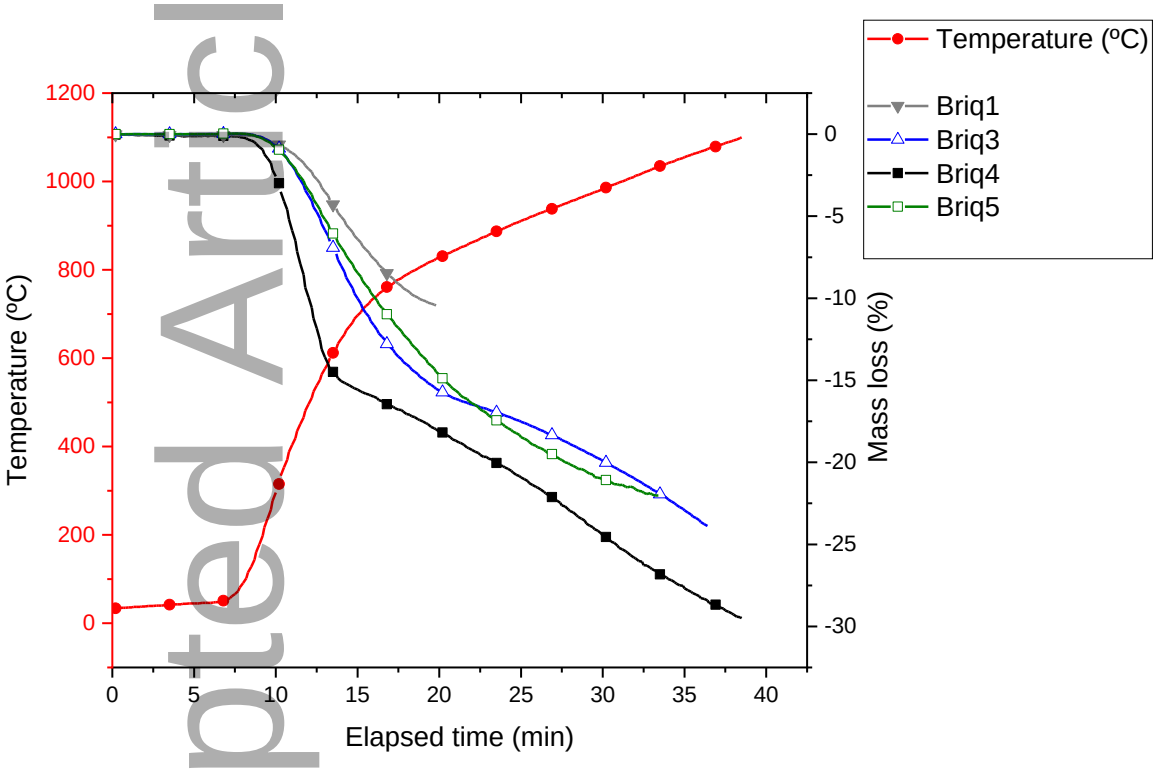

Figure 19: Mass loss and temperature profile for full briquettes reduced in a tube furnace.

(a) (b)

Figure 20: post-reduction of (a) complete BRIQ3 sample and (b) cut BRIQ4 sample.

It also appeared that shrinkage had taken place and that the volume of the BRIQ4 pieces was reduced. The dimensions of each part of the briquette and the mass loss are shown in Table 15 below. Similar to dilatometry results, size reduction is likely associated with iron oxides reduction.

Table 15: Mass loss and shrinkage of each briquette piece from BRIQ4.

Briquette piece	Mass reduction (%)	Volume reduction (%)
BRIQ4-1	32.88	39.97
BRIQ4-2	33.07	39.84
BRIQ4-3	33.27	41.66
BRIQ4-4	33.18	41.55
Average	33.10	

4.6.2. Characterization of samples after reduction trials

The residual briquettes obtained from the furnace trials were subjected to metallographic analysis. Different iron oxidation states were detected with different methods, and a summary of these results is presented in Table 16.

Table 16: Metallographic analysis of briquettes post reduction.

[%]	Fe total	Fe^{2+}	Fe-Met	$Fe3^{+}$
Analysis method	DIN EN ISO 11885. 2009-09	AM_EG.26 (Titration)	ISO 5416. 2006-04	Calculated
BRIQ1	44.9	12.3	0.25	32.35
BRIQ3	70.7	45.2	22.3	3.2
BRIQ4	81.3	26.6	47	7.7
BRIQ5	2.1	0.17	0.54	1.39

It can be observed that the iron in BRIQ1 was still in an unreduced state. This was due to trials having to stop at earlier stage and at lower temperatures. In samples BRIQ4 and BRIQ3, the reduction of iron was progressed. Comparison was carried out between the initial briquette iron and reduced briquette iron content form of FeO and Fe_2O_3 for simplicity. In practice, there is also a third phase of Fe_3O_4 that is a mixture between two and three valent iron oxide. The total amount of iron-bearing phases was normalized to one to account for moisture and binder vaporization in the reduction process. The degree of reduction in the briquette was calculated according to the loss of oxygen in the reduction.

BRIQ4 and BRIQ3 had a similar recipe composition. However, after the reduction trial of BRIQ4, the reduction degree was calculated to be 35.2%, while the reduction degree of BRIQ3 was 7.9%. The significantly higher reduction degree of BRIQ4 is attributed to the fact that quarters of the BRIQ4 were used in the reduction tests. However, a full briquette of BRIQ3 was used in the reduction test. These results confirm the crucial role that heat transfer played in the reduction of briquettes. With smaller briquette pieces, the core of the sample was heated relatively faster compared to the full

briquette sample, contributing to a higher reduction rate and extent, as indicated by Figure 19. Moreover, smaller pieces of the briquette correspond to a larger surface area exposed to reducing gases, which also played a role in enhancing the reduction rate.

The reducing behavior of the tested briquettes was also confirmed by XRD analysis (Figure 21 and Figure 22). The reduced BRIQ1 was mainly comprised of magnetite with a residual amount of hematite, and no metallic iron was detected. The results of the quantitative analysis conducted using the RIR method are in good agreement with those of the chemical analysis conducted to speciate iron compounds (Table 16). BRIQ3 and BRIQ4 showed an intense peak associated with iron formation that is visible although residual amounts of iron oxides and carbon (the halo centered at 25° 2Θ) exist. Additionally, the results of the quantitative analysis conducted using the RIR method are in the same order of magnitude as those of the speciation analysis (Table 16). However, BRIQ5 shows a lesser extent of reduction. Indeed, after thermal treatment, BRIQ5 is mainly formed by MnO and MnO_2. This means that the reduction of superior manganese oxide (Mn_3O_4) proceeded well, and this result agrees with the mass loss registered during furnace reduction trials. The reduction was less extensive than during TGA testing due to lower maximum temperature reached. RIR quantitative analysis was not performed on BRIQ5 because the phase arrangement is more complex than the other analyzed samples.

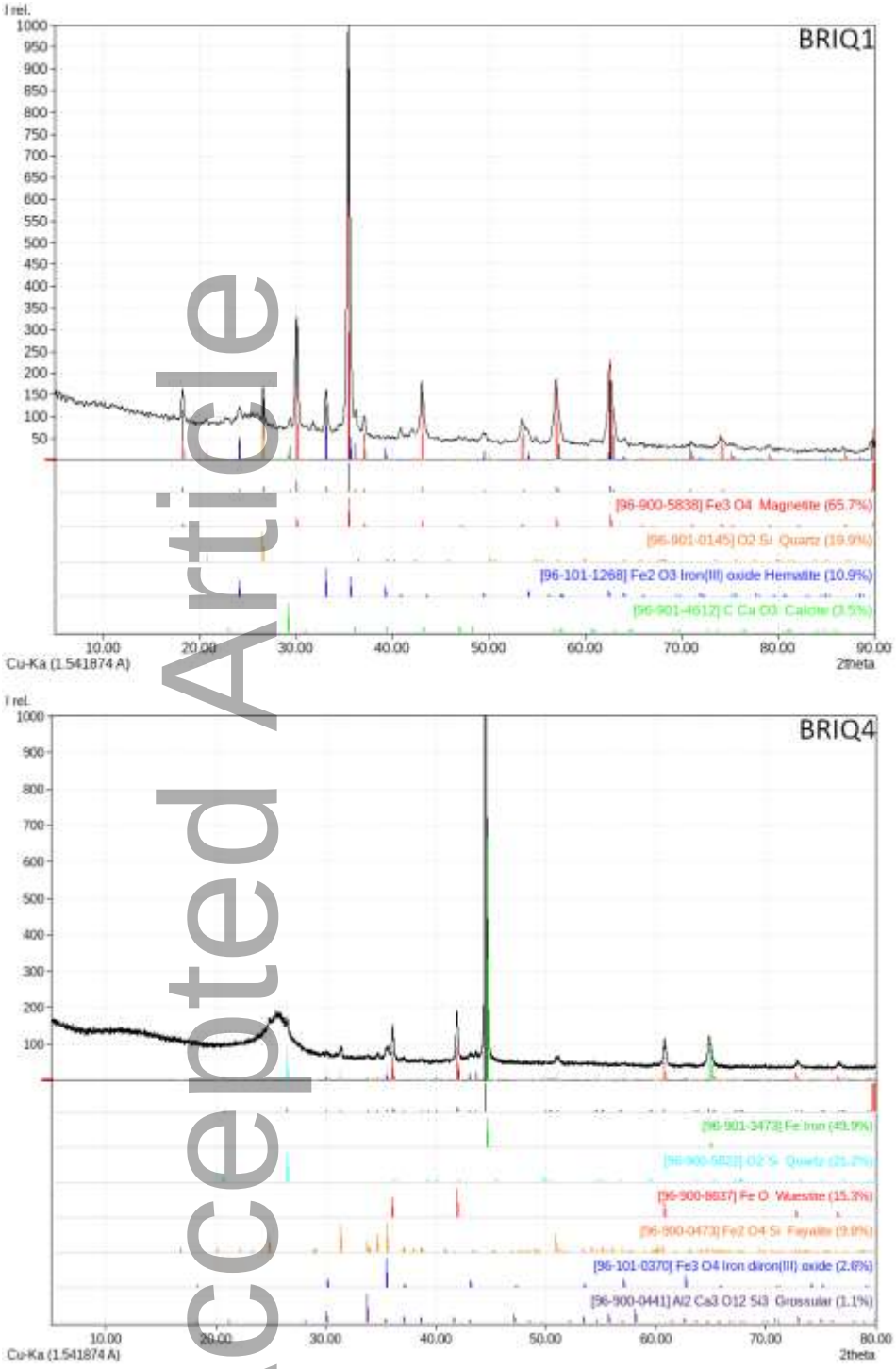

Figure 21: XRD pattern of reduced briquettes and RIR quantitative analysis for BRIQ1 and BRIQ4.

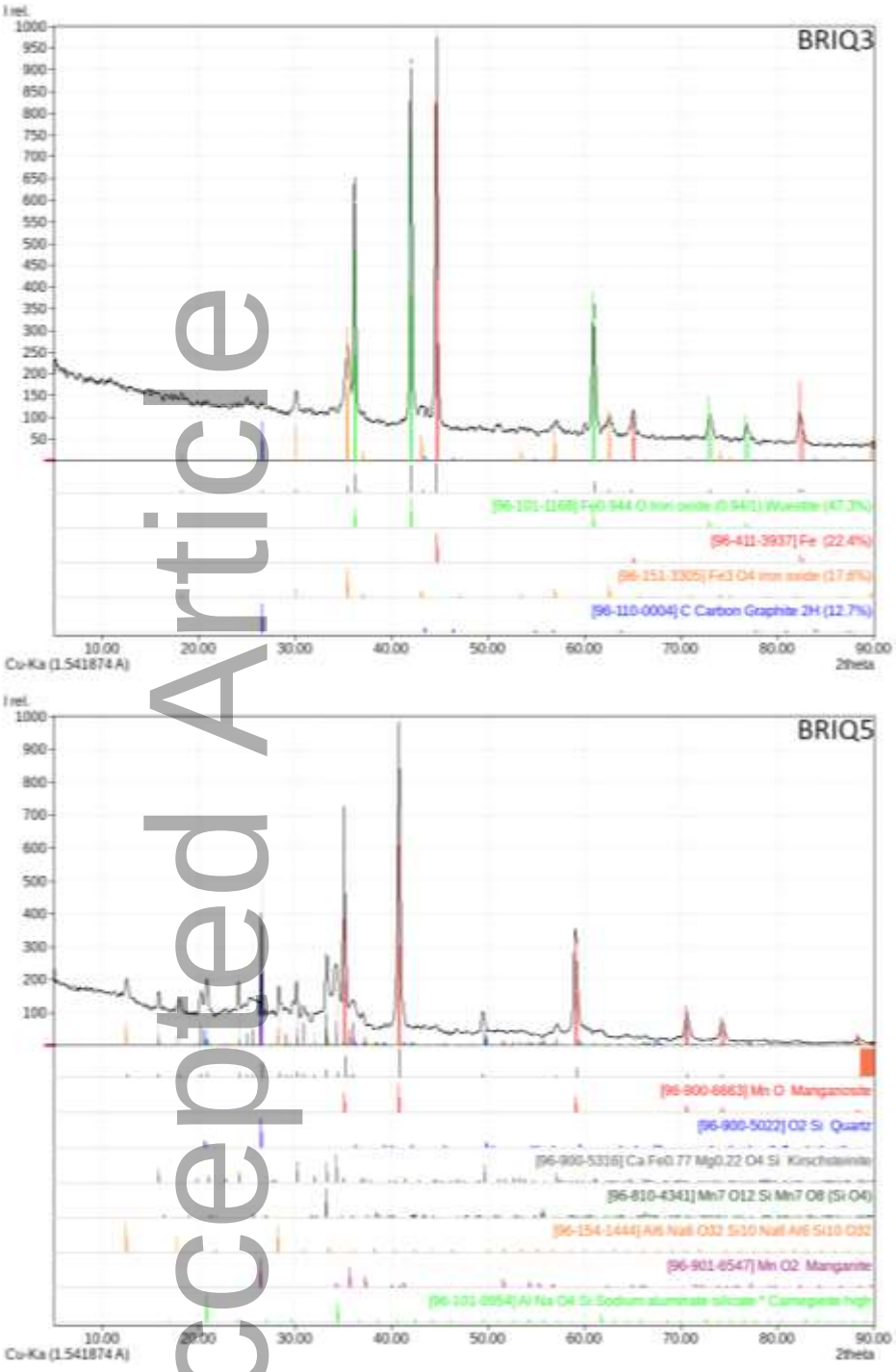

Figure 22: XRD pattern of reduced briquettes and RIR quantitative analysis for BRIQ3 and BRIQ5.

4.7. Evaluation of overall briquette performance

The briquettes' performance during each test, as well as their overall performance, is summarized in Table 17 below. The performance is assessed based on observations, values from literature and test results of reference material used in EAF such as ferroalloys and lime stones.

Table 17: Briquette performance evaluation indicated by + for suitable and ++ for excellent performance.

Test	Compression	Drop test	TGA-MS	Melting	Reduction	Dilatometry	Sample prep	Suitability
BRIQ1	++	+	+	NA	-	++	+	unsuitable
BRIQ2	+	-	+	NA	NA	+	+	unsuitable
BRIQ3	++	+	+	NA	+	++	+	suitable
BRIQ4	+	++	+	NA	++	++	+	suitable
BRIQ5	+	-	+	NA	+	-	-	unsuitable
BRIQ6	+	++	NA	++	NA	++	-	use limited
BRIQ7	+	++	NA	++	NA	++	-	use limited

After evaluating different briquettes by employing various testing techniques, BRIQ3 and 4 showed better behavior among self-reducing briquettes in tests simulating EAF conditions. As BRIQ1 developed heavy black fumes during the early stages of heating, it cannot be used in high quantities in an EAF. BRIQ5 performed poorly in dilatometry testing and showed a tendency toward low temperature disintegration, which indicates a risk for higher dust generation when used in an EAF. It also showed poor drop damage resistance which also pose a risk of fines generations during handling and charging.

Among the slag-forming briquettes, BRIQ6 and BRIQ7 were deemed suitable for use in an EAF due to their favorable melting characteristics. BRIQ2 was stable and did not melt completely at temperatures close to the EAF tapping temperature, which indicates a risk of clogging. However, BRIQ2 consisted mainly of CaO, which has high melting point but is known to dissolve into EAF slag, which suggests that there is no risk of the tapping hole becoming clogged. On the other hand, BRIQ2 performed very poorly drop in damage resistance after long storage time with briquettes surviving 3 drops or less, which makes it unsuitable for EAF in order to avoid risk for fines generation.

BRIQ5, BRIQ6, and BRIQ7 were sensitive to water upon contact during sample preparations, indicating that they may not withstand moisture or high humidity conditions upon storage prior to their use. Therefore, these briquettes can only be utilized if they are introduced to EAF soon after arriving at the site.

5. Conclusions

In this research, four recipes for self-reducing briquettes (BRIQ 1, 3, 4, and 5) and three recipes for slag-forming briquettes (BRIQ 2, 6, and 7) were tested for their suitability in EAF operations. Several tests were employed to simulate conditions that briquettes are subjected to prior to and during their use in an EAF. BRIQ1, BRIQ2, BRIQ3, BRIQ4, and BRIQ5 contained starch and paper fibers as a binder, while BRIQ6 employed only starch as a binder, and BRIQ7 employed sodium silicate as a binder. During the TGA-MS trials, MS peaks indicating water release were observed around 100 °C, Starch and fiber decomposition MS peaks took place at low temperature. The start of iron oxide reduction was observed around 550 °C, with reduction steps indicated by CO and CO_2 peaks around 750 °C and 900 °C.

The results indicate that the briquette recipes BRIQ3, BRIQ4, BRIQ6, and BRIQ7 can be deemed suitable for EAF charging. BRIQ1 produced high volatiles and thick black fumes when the full-scale recipe was tested, which makes its use challenging. BRIQ2 did not completely melt during dilatometry analysis at near-tapping temperatures, likely due to the presence of CaO, which would dissolve in the slag, and also showed poor drop damage resistance during testing. BRIQ5 crumbled at low temperatures during dilatometry testing, indicating a possible tendency toward low temperature disintegration during EAF operation.

During melting trials, BRIQ6's and BRIQ7's behavior was assessed while in contact with industrial slag melted at 1500 °C and were deemed suitable for EAF operations. However, difficulties were encountered while preparing BRIQ5, BRIQ6, and BRIQ7 samples when they came into contact with water, indicating their hydrophilic nature and possible difficulties upon their storage in moist or high humidity conditions.

Acknowledgement

This research is part of the Fines2EAF project and received funding from the Research Fund for Coal and Steel (RFCS) of the European Community with Grant Agreement No. 754197. Chemical and mineralogical characterizations were performed with the support of the Centre for Material Analysis, University of Oulu, Finland. The authors would like to acknowledge the technical assistance of Mr. Tommi Kokkonen from the Process Metallurgy research unit at the University of Oulu. The authors would also like to acknowledge the financial support from the Finnish Cultural Foundation (Grant number: 60212342/2021), Olvi Foundation, and Walter Ahlström foundation.

References

[1] Worldsteel association, 'WORLD STEEL IN FIGURES 2021', Belgium, **2021**.

[2] J. A. de Araújo, V. Schalch, *J. Mater. Res. Technol.* **2014**, *3*, 274, DOI: 10.1016/j.jmrt.2014.06.003.

[3] S. Ndlovu, G. S. Simate, E. Matinde, 'Waste Production and Utilization in the Metal Extraction Industry', CRC Press, Taylor & Francis Group, 6000 Broken Sound Parkway NW, Suite 300, Boca Raton, FL 33487-2742, **2017**, DOI: 10.1201/9781315153896.

[4] Y. Gordon, S. Kumar, *Trans. Indian Inst. Met.* **2013**, *66*, 501, DOI: 10.1007/s12666-013-0267-5.

[5] T. Suetens, K. Van Acker, B. Blanpain, B. Mishra, D. Apelian, *Miner. Met. Mater. Soc.* **2014**, *66*, 1119, DOI: 10.1007/s11837-014-1044-6.

[6] J.-T. Gao, S.-Q. Li, Y.-L. Zhang, Y.-T. Zhang, P.-Y. Chen, *Ironmak. Steelmak.* **2012**, *39*, 446, DOI: 10.1179/1743281211Y.0000000093.

[7] 'Resource Recovery and Recycling from Metallurgical Wastes', Elsevier, **2006**, DOI: 10.1016/S0713-2743(06)X8083-2.

[8] N. A. Godinskii, N. N. Kushnarev, D. S. Yakhshuk, V. I. Kotenev, E. Y. Barsukova, **2003**, *47*, 4.

[9] Y. N. Toulouevski, I. Y. Zinurov, 'Innovation in Electric Arc Furnaces', Springer Berlin Heidelberg, Berlin, Heidelberg, **2013**, DOI: 10.1007/978-3-642-36273-6.

[10] M. C. Bagatini, V. Zymla, E. Osório, A. C. F. Vilela, *ISIJ Int.* **2017**, *57*, 2081, DOI: 10.2355/isijinternational.ISIJINT-2017-242.

[11] A. Davydenko, A. Karasev, B. Glaser, P. Jönsson, *Materials* **2019**, *12*, 3434, DOI: 10.3390/ma12203434.

[12] A. Davydenko, A. Karasev, G. Lindstrand, P. Jönsson, *Steel Res. Int.* **2015**, *86*, 146, DOI: 10.1002/srin.201400036.

[13] Yang, Q., *Steel Res. Int.* **2009**, DOI: 10.2374/SRI09SP003.

[14] M. Geerdes, R. Chaigneau, I. Kurunov, O. Lingiardi, J. Ricketts, 'Modern Blast Furnace Ironmaking: An Introduction (Third Edition, 2015)', IOS Press, **2015**.

[15] British Standards Institution, 'Iron ore pellets for blast furnace and direct reduction feedstocks — Determination of the crushing strength (BS ISO 4700:2007)', British Standards Institution (BSI), London, **2008**.

[16] T. Echterhof, T. Willms, S. Preiss, M. Aula, A. Abdelrahim, T. Fabritius, D. Mombelli, C. Mapelli, S. Steinlechner, I. Unamuno, *Appl. Sci.* **2019**, *9*, 3946, DOI: 10.3390/app9193946.

[17] N. A. El-Hussiny, M. E. H. Shalabi, *Powder Technol.* **2011**, *205*, 217.

[18] A. Magdziarz, M. Ku, M. Hryniewicz, *Chem Process Eng* **2015**, 9.

[19] S. R. Richards, *Fuel Process. Technol.* **1990**, *25*, 89.

[20] D. S. Kumar, R. Sah, V. R. Sekhar, S. C. Vishwanath, *Ironmak. Steelmak.* **2017**, *44*, 134, DOI: 10.1080/03019233.2016.1165499.

[21] F. A. López, A. López-Delgado, *J. Environ. Eng.* **2002**, *128*, 1169, DOI: 10.1061/(ASCE)0733-9372(2002)128:12(1169).

[22] British Standards Institution, 'Iron ores for blast furnace and direct reduction feedstocks. Determination of the tumble and abrasion indices. (BS ISO 3271-2007)', British Standards Institution (BSI), London, **2007**.

[23] A.-G. Guézennec, J.-C. Huber, F. Patisson, P. Sessiecq, J.-P. Birat, D. Ablitzer, *Powder Technol.* **2005**, *157*, 2, DOI: 10.1016/j.powtec.2005.05.006.

[24] T. Jarnerud, A. V. Karasev, P. G. Jönsson, *Materials* **2019**, *12*, 2888, DOI: 10.3390/ma12182888.

[25] E. A. Mousa, H. M. Ahmed, C. Wang, *ISIJ Int.* **2017**, *57*, 1788, DOI: 10.2355/isijinternational.ISIJINT-2017-127.

[26] T. Demus, T. Reichel, M. Schulten, T. Echterhof, H. Pfeifer, *Ironmak. Steelmak.* **2016**, *43*, 564, DOI: 10.1080/03019233.2016.1168564.

[27] P. Paknahad, M. Askari, S. A. Shahahmadi, *J. Sustain. Metall.* **2019**, *5*, 497, DOI: 10.1007/s40831-019-00240-y.

[28] P. Derungs, J. M. Brouhon, G. Harp, 'Briquetting of self-reducing blendings of waste iron oxides mixture: final report', Off. For Off. Publ. Of The Europ. Communities, Luxembourg, **2002**.

[29] ASTM International, 'ASTM D440-07, Standard Test Method of Drop Shatter Test for Coal', ASTM International, West Conshohocken, PA, **2019**, DOI: 10.1520/D0440-07R19E01.

[30] ASTM International, 'ASTM D3038-93, Standard Test Method for Drop Shatter Test for Coke', ASTM International, West Conshohocken, PA, **2018**, DOI: 10.1520/D3038-93R18.

[31] M. J. Blesa, J. L. Miranda, M. T. Izquierdo, R. Moliner, *Fuel Process. Technol.* **2003**, *80*, 155, DOI: 10.1016/S0378-3820(02)00243-6.

[32] R. Sen, S. Wiwatpanyaporn, A. P. Annachhatre, *Int. J. Environ. Waste Manag.* **2016**, *17*, 158, DOI: 10.1504/IJEWM.2016.076750.

[33] J. R. Dankwah, P. Koshy, V. Sahajwalla, *Ironmak. Steelmak.* **2014**, *41*, 401, DOI: 10.1179/1743281213Y.0000000125.

[34] J. R. Dankwah, P. Koshy, P. O'Kane, V. Sahajwalla, *Steel Res. Int.* **2012**, *83*, 766, DOI: 10.1002/srin.201200019.

[35] J. R. Dankwah, P. Koshy, *High Temp. Mater. Process.* **2014**, *33*, 107, DOI: 10.1515/htmp-2013-0035.

[36] V. I. Babanin, A. Y. Eremin, G. N. Bezdezhskii, *Metallurgist* **2007**, *51*, 6.

[37] L. R. Lemos, S. H. F. S. da Rocha, L. F. A. de Castro, *J. Mater. Res. Technol.* **2015**, *4*, 278, DOI: 10.1016/j.jmrt.2014.12.002.

[38] British Standards Institution, 'Iron ores for blast furnace feedstocks Determination of low-temperature reduction disintegration indices by static method (BS ISO 4696:2007)', London, **2007**.

[39] British Standards Institution, 'Iron ores for blast furnace feedstocks- Determination of the decrepitation index. (BS ISO 8371:2015)', London, **2015**.

[40] S. Seetharaman, A. McLean, R. Guthrie, S. Sridhar, Eds. , 'Industrial processess', Elsevier, Amsterdam, **2014**.

[41] Commission of the European Union. Joint Research Centre. Institute for Prospective Technological Studies., 'Best available techniques (BAT) reference document for iron and

steel production: industrial emissions Directive 2010/75/EU : integrated pollution prevention and control.', Publications Office, LU, **2013**.

[42] A. Roine, 'HSC Chemistry®Ver. 8.1.4', Outotec Research Oy, Pori, Finland, **2014**.

[43] Q. Ye, G. Li, Z. Peng, R. Augustine, M. D. Pérez, Y. Liu, M. Liu, M. Rao, Y. Zhang, T. Jiang, *Powder Technol.* **2020**, *362*, 781, DOI: 10.1016/j.powtec.2019.10.108.

[44] T. Willms, T. Echterhof, S. Steinlechner, M. Aula, A. Abdelrahim, T. Fabritius, D. Mombelli, C. Mapelli, S. Preiss, *Appl. Sci.* **2020**, *10*, 8309, DOI: 10.3390/app10228309.

[45] C. Takano, R. C. Nascimento, G. F. B. L. e Silva, D. M. dos Santos, M. B. Mourão, J. D. T. Capocchi, *Mater. Trans.* **2001**, *42*, 2506, DOI: 10.2320/matertrans.42.2506.

[46] Technical Committee CEN/TC 292, 'EN 14346:2006, Characterization of waste - Calculation of dry matter by determination of dry residue or water content', **2006**.

[47] British Standards Institution, 'Tests for mechanical and physical properties of aggregates. Part 3: Determination of loose bulk density and voids (BS EN 1097 :1998)', British Standards Institution (BSI), London, **1998**.

[48] British Standards Institution, 'Tests for mechanical and physical properties of aggregates. Part 7: Determination of the particledensity of filler — Pyknometer method (BS EN 1097-7:2008)', British Standards Institution (BSI), London, **2009**.

[49] M. Singh, B. Bjorkman, *Miner. Metall. Process.* **2006**, *23*, 203.

[50] M. Singh, Ph.D. Thesis Luleå University of Technology, **2003**.

[51] W. Pietsch, 'Agglomeration processes: phenomena, technologies, equipment', Wiley-VCH, Weinheim, **2002**.

[52] Y. Leng, 'Materials characterization: introduction to microscopic and spectroscopic methods', Wiley-VCH, Weinheim, **2013**.

[53] P. K. Gallagher, M. E. Brown, R. B. Kemp, Eds. , 'Handbook of thermal analysis and calorimetry', Elsevier, Amsterdam [Netherlands] ; New York, **1998**.

[54] A. Abdelrahim, M. Iljana, M. Omran, T. Vuolio, H. Bartusch, T. Fabritius, *ISIJ Int.* **2020**, DOI: 10.2355/isijinternational.ISIJINT-2019-734.

[55] Y. Liu, L. Yang, C. Ma, Y. Zhang, *Materials* **2019**, *12*, 699, DOI: 10.3390/ma12050699.

[56] R. Cypres, C. Soudan-Moinet, *Fuel* **1980**, *59*, 48, DOI: 10.1016/0016-2361(80)90010-1.

[57] R. Cyprès, C. Soudan-Moinet, *Fuel* **1981**, *60*, 33, DOI: 10.1016/0016-2361(81)90028-4.

Table of content text

In this paper, testing techniques are used to assess the suitability of briquettes in EAF operations. Self-reducing and slag-forming briquettes utilizing different binders were tested. Charging, heating, and melting behavior were assessed. Three briquettes were deemed suitable for use in EAF operations, while two briquettes were deemed of limited use, and two briquettes were deemed unsuitable.